Int. J. Anal. Appl. (2024), 22:160

International Journal of Analysis and Applications

Modeling of KSHV/HHV-8 and HIV-1 Co-Dynamics in Vivo

E. A. Almohaimeed[1,2], A. M. Elaiw[1,*], A. D. Hobiny[1]

[1]*Department of Mathematics, Faculty of Science, King Abdulaziz University, P. O. Box 80203, Jeddah 21589, Saudi Arabia*

[2]*Department of Mathematics, College of Science, Qassim University, P.O. Box 53, Buraydah 51921, Saudi Arabia*

[*]*Corresponding author:* aelaiwksu.edu.sa@kau.edu.sa

Abstract. Human immunodeficiency virus kind 1 (HIV-1) compromises the immune system by infecting and damaging $CD4^+$ T cells. Infection can progress to the ultimate stage, acquired immune deficiency syndrome (AIDS), if HIV-1 therapy is not received. People living with HIV/AIDS are more vulnerable to infections that they otherwise wouldn't develop. Opportunistic infections or malignancies are the terms used to describe them. Kaposi sarcoma (KS) is an AIDS-related malignancy caused by Kaposi's sarcoma-associated herpesvirus (KSHV) (also known as human herpesvirus 8 (HHV-8)). HIV-1 and KSHV co-infection cases has been shown in several studies. Using a system of ODEs, we develop a new mathematical model to study the co-dynamics of HIV-1 and KSHV in vivo. The model includes interactions between healthy $CD4^+$ T cells, HIV-1-infected $CD4^+$ T cells, HIV-1 particles, healthy B cells, KSHV-infected B cells, and KSHV particles. By analyzing the boundedness and nonnegativity of the solutions, we prove the mathematical well-posedness and biological compatibility of the model. The existence and stability of the model's steady states are established by four threshold values that we identify. We prove that steady states are globally asymptotically stable by using Lyapunov's method and LaSalle's invariance principle. Numerical simulations are used to display the results. For both basic reproduction ratios of HIV-1 mono-infection (R_1) and KSHV mono-infection (R_2), sensitivity analysis is carried out. A comparison between HIV-1 or KSHV mono-infections and co-infections with HIV-1 and KSHV is given. Empirical evidence indicates that co-infection results in higher KSHV and HIV-1 concentrations compared to mono-infection cases. This result is in line with a number of findings found in the literature.

1. Introduction

One of the biggest clinical challenges is persistent viral infections such as those caused by hepatitis B or C virus (HBV or HCV), human immunodeficiency virus kind 1 (HIV-1) and human cytomegaly virus (HCMV). HIV-1 is harmful because it may damage several immune cell types,

Received: Jul. 23, 2024.

2020 *Mathematics Subject Classification.* 92D30.

Key words and phrases. co-infection; HIV-1; KSHV/HHV-8; global stability; Lyapunov function.

https://doi.org/10.28924/2291-8639-22-2024-160
ISSN: 2291-8639

including monocytes, dendritic cells, macrophages, and $CD4^+$ T cells [1], [2]. Nonetheless, $CD4^+$ T cells are thought to be HIV-1's primary target. The immune system's innate and adaptive components work together to protect the body against outside invaders. Cellular immunity and humoral immunity make up adaptive immunity [2]. B cells are the foundation of humoral immunity because they produce a specific antibody that directly neutralizes the virus. Cytotoxic T-lymphocytes (CTLs) are the building blocks of cellular immunity; they eliminate the infected cells [3]. Single-stranded RNA virus HIV-1 is a member of the Retroviridae family of viruses. In addition, HIV-1 is a lentivirus, a kind of retrovirus that infects host cells over a long period of time by progressively destroying them [2]. When the $CD4^+$ T cell count of an HIV-1 infected individual falls below a certain threshold (200 cells/mm^3), the condition is known as acquired immune deficiency syndrome (AIDS) [4]. Then the body becomes vulnerable to many opportunistic infections including STDs (sexually transmitted diseases), respiratory infections, and some tumors. Semen, Blood, vaginal secretions and breast milk, are among the bodily fluids via which HIV-1 may transmit [5].

One of the AIDS-related diseases is Kaposi sarcoma (KS) which is a type of cancer [6]. KS is caused by Kaposi's sarcoma-associated herpesvirus (KSHV) (also known as human herpesvirus 8 (HHV-8)). KSHV is first discovered by Chang et al. [7] which is a member of the Herpesviridae family of DNA viruses. KSHV may infect a variety of cell types, such as macrophages, endothelial cells, B cells, and epithelial cells [8]. But B cells are the main target of KSHV [9]. KSHV has been shown to be transmissible by a variety of routes, such as blood products, sexual contact and salivary shedding [10]. Healthy people who test positive for KSHV have a very low probability of developing KS. The danger is substantially larger for those with impaired immune systems, though [11]. According to a report in [12], individuals with HIV-1 have a higher likelihood of becoming KSHV seropositive than those without HIV-1. Numerous studies documented occurrences of co-infection between HIV-1 and KSHV (see e.g., [13], [14], [15], [16]. [17], [18]).

Our knowledge of viral dynamics has significantly increased thanks to rigorous mathematical modeling and analysis, which can help us come up with workable and efficient management plans to eradicate viral infections. One of the areas of mathematical immunology that is progressing the fastest is the formulation of mathematical models of the dynamics of HIV-1 infection. Three populations are included in the classic model of HIV-1 mono-infection [19]: healthy $CD4^+$ T cells, infected cells, and free HIV-1 particles. Later on, the model was extended in a great deal of publications to include other biological elements such as time delay [20], [21], [22], [23], cell-to-cell transmission [24], [25], [26], [27], reaction-diffusion [25], [28], latently infected cells [28], [29], [30], cellular immune response [19], [26], [31], humoral immune response [24], [32], [33], both cellular and humoral immune responses [34], [35], [36], age-structured [27], [37], [38] and antiretroviral treatment [39], [40], [41].

Researchers haven't paid much attention to modeling the dynamics of an KSHV mono-infection in vivo. The three primary components of the KSHV infection model are healthy B cells, infected B cells, and free KSHV particles. Chimbola et al. [42] formulated a KSHV mono-infection model.

Only the healthy steady state's stability was examined, though. A mathematical model developed by Nani and Jin [43] depicts the progression of HIV-1 co-infection and KS under the influence of highly active antiretroviral treatment (HAART). The same authors in [44] added adoptive cellular immunotherapy to strengthen this model. However, these two publications omitted information about the kinematics of free KSHV particles as well as B cells. In [10], [45] and [46], models were developed to show how co-infection with HIV-1 and KSHV progresses. The healthy $CD4^+$ T cells and healthy B cells were not taken into consideration by the model in [10]. Except for examining the positivity of the solutions, the model in [45] was not mathematically examined. In [10] and [46], the investigation focused solely on the stability of the healthy steady state. We further observe that the models shown in [10], [43], [44], [45] and [46] ignored the function of B cells in the fight against HIV-1.

In this work, we present a novel model of KSHV/HIV-1 co-dynamics in vivo. B cells' defense against HIV-1 is included in the model. Apart from the global stability of the steady states, we investigate the fundamental characteristics of the solutions to the model. The global stability of the four steady states are proven by using Lyapunov's approach and applying LaSalle's invariance principle. In order to verify the theoretical findings, we offer numerical simulations. We carry out sensitivity analysis for the basic reproduction ratios of HIV-1 mono-infection (R_1) and KSHV mono-infection (R_2). We conclude by discussing the results. Our model and its analysis may be important to study the dynamics of different human viruses.

2. Model formulation

In this section, a KSHV/HIV-1 co-infection model is introduced. The dynamics of KSHV/HIV-1 co-infection is illustrated in Figure 1. We develop our suggested model based on the following presumptions:

- A1 Six populations are depicted in the model: healthy $CD4^+$ T cells (U), HIV-1-infected $CD4^+$ T cells (Y), HIV-1 particles (V), healthy B cells (W), KSHV-infected B cells (Z), and KSHV particles (P).
- A2 HIV-1 and KSHV target healthy $CD4^+$ T cells and B cells, respectively.
- A3 The rate at which healthy $CD4^+$ T cells are produced is ξ, they die at ϖU, and they get HIV-1 infection at ϱUV.
- A4 The mortality rate of $CD4^+$ T cells infected with HIV-1 is δY.
- A5 At rate $\varkappa Y$, HIV-1-infected $CD4^+$ T cells create the HIV-1 particles, which are then eliminated at rate ϑV.
- A6 At the rate of ρWV, the antibodies (generated by B cells) neutralize HIV-1 particles.
- A7 The rate of generation of healthy B cells is ℓ, whereas the rate of simulation by HIV-1 is κWV, the rate of mortality is βW, and the rate of infection by KSHV is νPW.
- A8 The rate of mortality of KSHV-infected B cells is ηZ.

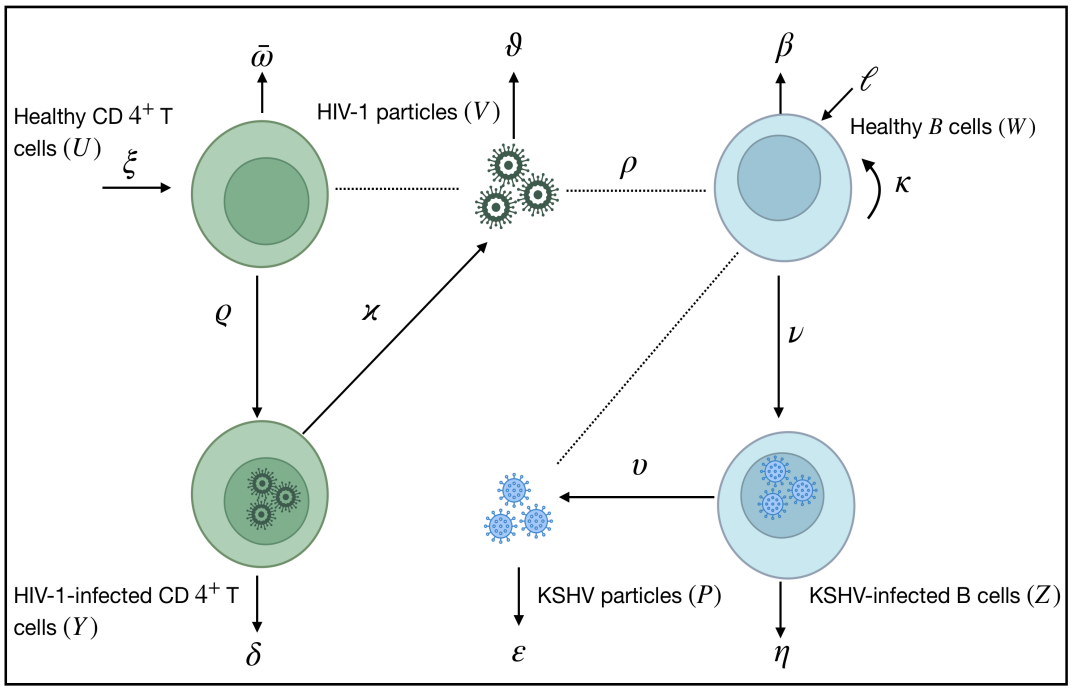

FIGURE 1. The schematic illustration of the HIV-1 and KSHV co-dynamics concept.

A9 At a rate of υZ, KSHV-infected B cells create KSHV particles, which thereafter die at a rate of εP.

Here, we denote the concentrations of the compartments at time t by $U = U(t)$, $Y = Y(t)$, $V = V(t)$, $W = W(t)$, $Z = Z(t)$ and $P = P(t)$. The above assumptions lead us to formulate the following system:

$$\dot{U} = \xi - \bar{\omega}U - \varrho UV, \tag{2.1}$$

$$\dot{Y} = \varrho UV - \delta Y, \tag{2.2}$$

$$\dot{V} = \varkappa Y - \vartheta V - \rho WV, \tag{2.3}$$

$$\dot{W} = \ell + \kappa WV - \beta W - \nu PW, \tag{2.4}$$

$$\dot{Z} = \nu PW - \eta Z, \tag{2.5}$$

$$\dot{P} = \upsilon Z - \varepsilon P. \tag{2.6}$$

All presented parameters of model (2.1)-(2.6) are positive. The description and value of the parameters are presented in Table 1. Some of the parameters's value are taken from previous studies, while other values are assumed.

TABLE 1. Model parameters.

Symbol	Parameter	Value	Source
ξ	Source of healthy CD4$^+$T cells	10 cells mm^{-3} day^{-1}	[47]
ϖ	Mortality rate of healthy CD4$^+$T cells	0.01 day^{-1}	[48]
ϱ	Incidence rate of healthy CD4$^+$T cells by HIV-1	varied	
δ	Mortality rate of HIV-1-infected CD4$^+$T cells	0.4 day^{-1}	[47]
$\varkappa$	Generation rate of HIV-1 by infected CD4$^+$T cells	38 viruses cells^{-1} day^{-1}	[48]
ϑ	Mortality rate of HIV-1	2.4 day^{-1}	[48]
ρ	Neutralization rate of HIV-1 particles due to B cells	0.1 cells^{-1} mm^3 day^{-1}	
ℓ	Source of healthy B cells	48 cells mm^{-3} day^{-1}	[45]
κ	Activation rate of B cells	0.01 viruses^{-1} mm^3 day^{-1}	[49]
β	Mortality rate of healthy B cells	0.24 day^{-1}	[50]
ν	Incidence rate of healthy B cells by KSHV	varied	
η	Mortality rate of KSHV-infected B cells	0.33 day^{-1}	[50]
υ	Generation rate of KSHV particles by infected B cells	1 viruses cells^{-1} day^{-1}	Assumed
ε	Mortality rate of KSHV	0.57 day^{-1}	[45, 50]

3. Basic properties

We ensure the well-posedness of model (2.1)-(2.6) by providing the non-negativity and boundedness of solutions in this part. In addition, we compute all steady states with the associated threshold parameters.

3.1. Properties of the model's solutions.

We demonstrate the model's biological acceptability and mathematical well-posedness by examining the solutions' boundedness and nonnegativity.

Lemma 3.1. *All system's solutions are non-negative and bounded.*

Proof. From Eqs. (2.1)-(2.6) we have

$$\begin{aligned}
\dot{U}|_{U=0} &= \xi > 0, \\
\dot{Y}|_{Y=0} &= \varrho UV \geq 0, \qquad \forall V, U \geq 0, \\
\dot{V}|_{V=0} &= \varkappa Y \geq 0, \qquad \forall Y \geq 0, \\
\dot{W}|_{W=0} &= \ell > 0, \\
\dot{Z}|_{Z=0} &= \nu PW \geq 0, \qquad \forall W, P \geq 0, \\
\dot{P}|_{P} &= = \upsilon Z \geq 0, \qquad \forall Z \geq 0.
\end{aligned}$$

Thus, according to Proposition B.7 of [51]

$$(U, Y, V, W, Z, P)(t) \in \mathbb{R}^6_+ \text{ for any } t \geq 0 \text{ when } (U, Y, V, W, Z, P)(0) \in \mathbb{R}^6_+.$$

Let's demonstrate the boundedness of solutions now. We define a function $\phi(t)$ as:

$$\phi = U + Y + \frac{\delta}{2\varkappa} V + \frac{\delta\rho}{2\varkappa\kappa} [W + Z] + \frac{\delta\eta\rho}{4\varkappa\upsilon\kappa} P.$$

Then, we get

$$\begin{aligned}
\dot{\phi} &= \dot{U} + \dot{Y} + \frac{\delta}{2\varkappa}\dot{V} + \frac{\delta\rho}{2\varkappa\kappa}\left[\dot{W} + \dot{Z}\right] + \frac{\delta\eta\rho}{4\varkappa\upsilon\kappa}\dot{P} \\
&= \xi - \omega U - \varrho UV + \varrho UV - \delta Y + \frac{\delta}{2\varkappa}\left[\varkappa Y - \vartheta V - \rho WV\right] + \frac{\delta\rho}{2\varkappa\kappa}\left[\ell + \kappa VW - \beta W - \nu PW\right. \\
&\left. + \nu PW - \eta Z\right] + \frac{\delta\eta\rho}{4\varkappa\upsilon\kappa}\left[\upsilon Z - \varepsilon P\right] \\
&= \xi + \frac{\delta\rho\ell}{2\varkappa\kappa} - \omega U - \frac{\delta}{2}Y - \frac{\delta\vartheta}{2\varkappa}V - \frac{\delta\rho\beta}{2\varkappa\kappa}W - \frac{\delta\eta\rho}{4\varkappa\kappa}Z - \frac{\delta\eta\rho\varepsilon}{4\varkappa\upsilon\kappa}P \\
&\leq \xi + \frac{\delta\rho\ell}{2\varkappa\kappa} - \sigma\left[U + Y + \frac{\delta}{2\varkappa}V + \frac{\delta\rho}{2\varkappa\kappa}(W + Z) + \frac{\delta\eta\rho}{4\varkappa\upsilon\kappa}P\right] \\
&= \xi + \frac{\delta\rho\ell}{2\varkappa\kappa} - \sigma\phi,
\end{aligned}$$

where $\sigma = \min\{\omega, \delta/2, \vartheta, \beta, \eta/2, \varepsilon\}$. Thus,

$$\phi(t) \leq \frac{\xi}{\sigma} + \frac{\delta\rho\ell}{2\varkappa\kappa\sigma} = \theta_1 \qquad \text{if} \qquad \phi(0) \leq \theta_1.$$

It follows that

$$0 \leq U(t), Y(t) \leq \theta_1,\ 0 \leq V(t) \leq \theta_2,\ 0 \leq W(t), Z(t) \leq \theta_3,\ 0 \leq P(t) \leq \theta_4$$

if

$$U(0) + Y(0) + \frac{\delta}{2\varkappa}V(0) + \frac{\delta\rho}{2\varkappa\kappa}\left[W(0) + Z(0)\right] + \frac{\delta\eta\rho}{4\varkappa\upsilon\kappa}P(0) \leq \theta_1$$

where $\theta_2 = \frac{2\varkappa}{\delta}\theta_1$, $\theta_3 = \frac{2\varkappa\kappa}{\delta\rho}\theta_1$ and $\theta_4 = \frac{4\varkappa\upsilon\kappa}{\delta\eta\rho}\theta_1$. □

3.2. **Steady states and thresholds.**

Lemma 3.2. *For system* (2.1)-(2.6)*, there exist four steady states as well as four thresholds* ($R_i, i = 1, 2, 3, 4$) *such that*

(I) *There is always an healthy steady state,* $SS_0 = (U_0, 0, 0, W_0, 0, 0)$.

(II) *When* $R_1 > 1$*, then there exists an KSHV mono-infection steady state,* $SS_1 = (U_1, 0, 0, W_1, Z_1, P_1)$*, in addition to* SS_0.

(III) *When* $R_2 > 1$*, then there exists an HIV-1 mono-infection steady state,* $SS_2 = (U_2, Y_2, V_2, W_2, 0, 0)$*, in addition to* SS_0.

(IV) *When* $R_3 > 1$ *and* $R_4 > 1$*, then then there exists an KSHV/HIV-1 co-infection steady state,* $SS_3 = (U_3, Y_3, V_3, W_3, Z_3, P_3)$*, in addition to* SS_0.

Proof. Steady states of (2.1)-(2.6) satisfy

$$\begin{cases} 0 = \xi - \omega U - \varrho UV, \\ 0 = \varrho UV - \delta Y, \\ 0 = \varkappa Y - \vartheta V - \rho WV, \\ 0 = \ell + \kappa WV - \beta W - \nu PW, \\ 0 = \nu PW - \eta Z, \\ 0 = \upsilon Z - \varepsilon P. \end{cases}$$

These equations provide four steady states:

(1) Healthy steady state, $SS_0 = (U_0, 0, 0, W_0, 0, 0)$, where $U_0 = \frac{\xi}{\omega}$ and $W_0 = \frac{\ell}{\beta}$.

(2) KSHV mono-infection steady state, $SS_1 = (U_1, 0, 0, W_1, Z_1, P_1)$, where

$$U_1 = \frac{\xi}{\omega}, W_1 = \frac{\eta\varepsilon}{\upsilon\nu} = \frac{W_0}{R_1}, Z_1 = \frac{\varepsilon\beta}{\upsilon\nu}(R_1 - 1), P_1 = \frac{\beta}{\nu}(R_1 - 1),$$

where

$$R_1 = \frac{\ell\upsilon\nu}{\eta\varepsilon\beta},$$

is the basic reproduction ratio for KSHV mono-infection. R_1 is known as the number of newly KSHV-infected B cells that result from one KSHV-infected B cell at the start of an KSHV mono-infection. A KSHV mono-infection can be established or not based on the parameter R_1.

(3) HIV-1 mono-infection steady state, $SS_2 = (U_2, Y_2, V_2, W_2, 0, 0)$, where

$$U_2 = \frac{\delta Y_2}{\varrho V_2}, Y_2 = \frac{\vartheta V_2 + \rho V_2 W_2}{\varkappa}, W_2 = \frac{\ell}{\beta - \kappa V_2}$$

and V_2 satisfies the following:

$$\frac{\omega_1 V^2 + \omega_2 V + \omega_3}{\beta - \kappa V} = 0,$$

where

$$\begin{aligned} \omega_1 &= \delta\vartheta\varrho\kappa, \\ \omega_2 &= \delta\omega\vartheta\kappa - \xi\varkappa\varrho\kappa - \delta\vartheta\varrho\beta - \delta\rho\ell\varrho, \\ \omega_3 &= \xi\varkappa\varrho\beta - \delta\omega\vartheta\beta - \delta\omega\rho\ell. \end{aligned}$$

We define a function $\Psi(V)$ as:

$$\Psi(V) = \frac{\omega_1 V^2 + \omega_2 V + \omega_3}{\beta - \kappa V}, \quad V \in \left(0, \frac{\beta}{\kappa}\right).$$

Note that, Ψ is continuous on $\left(0, \frac{\beta}{\kappa}\right)$. We have

$$\begin{aligned}\Psi(0) &= \frac{\xi\varkappa\varrho\beta - \delta\omega\vartheta\beta - \delta\omega\rho\ell}{\beta} \\ &= \frac{\delta\omega\vartheta\beta + \delta\omega\rho\ell}{\beta}\left(R_2 - 1\right)\end{aligned}$$

where

$$R_2 = \frac{\xi\varkappa\varrho\beta}{\delta\omega\left(\vartheta\beta + \rho\ell\right)},$$

which denotes the basic reproduction ratio for HIV-1 mono-infection. R_2 is known as the number of newly HIV-1-infected CD4$^+$T cells that result from one HIV-1-infected CD4$^+$T cell at the start of an HIV-1 mono-infection. An HIV-1 mono-infection can be established or not based on the parameter R_2.

Therefore, $\Psi(0) > 0$ if $R_2 > 0$. Moreover, we have $\lim\limits_{V \to \left(\frac{\beta}{\kappa}\right)^-} \Psi(V) = -\infty$. Thus, there exists V_2 such that $0 < V_2 < \frac{\beta}{\kappa}$ and satisfies $\Psi(V_2) = 0$. Consequently, $U_2 > 0,\ Y_2 > 0$ and $W_2 > 0$.

(4) KSHV/HIV-1 co-infection steady state, $SS_3 = (U_3, Y_3, V_3, W_3, Z_3, P_3)$, where

$$U_3 = \frac{\delta(\vartheta\upsilon\nu + \eta\varepsilon\rho)}{\varkappa\upsilon\nu\varrho},\ Y_3 = \frac{\omega(\vartheta\upsilon\nu + \eta\varepsilon\rho)}{\varkappa\upsilon\nu\varrho}\left(R_3 - 1\right),\ V_3 = \frac{\omega}{\varrho}\left(R_3 - 1\right),$$

$$W_3 = \frac{\eta\varepsilon}{\upsilon\nu},\ Z_3 = \frac{\varepsilon(\omega\kappa + \varrho\beta)}{\upsilon\nu\varrho}\left(R_4 - 1\right),\ P_3 = \frac{\omega\kappa + \varrho\beta}{\nu\varrho}\left(R_4 - 1\right),$$

where

$$\begin{aligned}R_3 &= \frac{\xi\varkappa\upsilon\nu\varrho}{\delta\omega(\vartheta\upsilon\nu + \eta\varepsilon\rho)}, \\ R_4 &= \frac{\upsilon\nu\varrho}{\omega\kappa + \varrho\beta}\left(\frac{\ell}{\eta\varepsilon} + \frac{\varkappa\kappa\xi}{\delta\left(\vartheta\upsilon\nu + \eta\varepsilon\rho\right)}\right).\end{aligned}$$

Therefore, the co-infection steady state, SS_3, exist if $R_3 > 1$ and $R_4 > 1$. In this case, the threshold values R_3 and R_4 indicate whether HIV-1 and KSHV co-infection is likely to occur. We note that, R_4 can be written as:

$$\begin{aligned}R_4 &= \frac{\ell\upsilon\nu\varrho\beta}{\eta\varepsilon\beta(\omega\kappa + \varrho\beta)} + \frac{\varkappa\upsilon\kappa\xi\nu\varrho\omega}{\delta\omega\left(\vartheta\upsilon\nu + \eta\varepsilon\rho\right)(\omega\kappa + \varrho\beta)} \\ &= R_1\frac{\varrho\beta}{\omega\kappa + \varrho\beta} + R_3\frac{\kappa\omega}{\omega\kappa + \varrho\beta} < R_1 + R_3,\end{aligned}$$

which leads to $R_4 < R_1$ as well as $R_4 < R_3$. The four threshold parameters are given as follows:

$$R_1 = \frac{\ell \upsilon \nu}{\eta \varepsilon \beta},$$
$$R_2 = \frac{\xi \varkappa \varrho \beta}{\delta \varpi \left(\vartheta \beta + \rho \ell\right)},$$
$$R_3 = \frac{\xi \varkappa \upsilon \nu \varrho}{\delta \varpi (\vartheta \upsilon \nu + \eta \varepsilon \rho)},$$
$$R_4 = \frac{\upsilon \nu \varrho}{\varpi \kappa + \varrho \beta}\left(\frac{\ell}{\eta \varepsilon} + \frac{\varkappa \kappa \xi}{\delta \left(\vartheta \upsilon \nu + \eta \varepsilon \rho\right)}\right).\square$$

4. Global stability

Here, the Lyapunov approach described in [52] will be used to investigate the four steady states of model's global asymptotic stability. We utilize the below-depicted arithmetic mean-geometric mean inequality

$$\sqrt[n]{\prod_{i=1}^{n} g_i} \leq \frac{1}{n}\sum_{i=1}^{n} g_i, \quad g_i \geq 0, \quad i = 1, 2, \ldots, n. \tag{4.1}$$

Let Λ_i be the Lyapunov function candidate and define T_i' as the largest invariant set of

$$T_i = \left\{(U, Y, V, W, Z, P) : \frac{d\Lambda_i}{dt} = 0\right\}, \qquad i = 0, 1, 2, 3.$$

Theorem 4.1. *The healthy steady state SS_0 is globally asymptotically stable (GAS) when $R_1 \leq 1$ and $R_2 \leq 1$. Moreover, SS_0 is unstable when $R_1 > 1$ and/or $R_2 > 1$.*

Proof. Define $\Lambda_0(U, Y, V, W, Z, P)$ as:

$$\Lambda_0 = U_0 \mathcal{L}\left(\frac{U}{U_0}\right) + Y + \frac{\delta}{\varkappa} V + \frac{\delta \rho}{\varkappa \kappa} W_0 \mathcal{L}\left(\frac{W}{W_0}\right) + \frac{\delta \rho}{\varkappa \kappa} Z + \frac{\delta \eta \rho}{\varkappa \upsilon \kappa} P,$$

where $\mathcal{L}(x) = x - \ln x - 1$. Obviously, $\Lambda_0(U, Y, V, W, Z, P) > 0$ for any $U, Y, V, W, Z, P > 0$ and $\Lambda_0(U_0, 0, 0, W_0, 0, 0) = 0$. Determining $\frac{d\Lambda_0}{dt}$ along the solutions of model (2.1)-(2.6) as:

$$\frac{d\Lambda_0}{dt} = \left(1 - \frac{U_0}{U}\right)\dot{U} + \dot{Y} + \frac{\delta}{\varkappa}\dot{V} + \frac{\delta \rho}{\varkappa \kappa}\left(1 - \frac{W_0}{W}\right)\dot{W} + \frac{\delta \rho}{\varkappa \kappa}\dot{Z} + \frac{\delta \eta \rho}{\varkappa \upsilon \kappa}\dot{P}.$$

Using equations of model (2.1)-(2.6), we obtain

$$\begin{aligned}\frac{d\Lambda_0}{dt} =& \left(1 - \frac{U_0}{U}\right)(\xi - \varpi U - \varrho U V) + (\varrho U V - \delta Y) + \frac{\delta}{\varkappa}\left(\varkappa Y - \vartheta V - \rho V W\right) \\ &+ \frac{\delta \rho}{\varkappa \kappa}\left(1 - \frac{W_0}{W}\right)(\ell + \kappa W V - \beta W - \nu P W) + \frac{\delta \rho}{\varkappa \kappa}\left(\nu P W - \eta Z\right) + \frac{\delta \eta \rho}{\varkappa \upsilon \kappa}\left(\upsilon Z - \varepsilon P\right).\end{aligned}$$

Collecting term and using $\xi = \varpi U_0$ and $\ell = \beta W_0$, we get

$$\begin{aligned}\frac{d\Lambda_0}{dt} =& \frac{-\varpi}{U}\left(U - U_0\right)^2 + \varrho U_0 V - \frac{\delta \vartheta}{\varkappa} V - \frac{\delta \rho}{\varkappa \kappa}\frac{\beta}{W}\left(W - W_0\right)^2 - \frac{\delta \rho}{\varkappa} W_0 V + \frac{\delta \rho \nu}{\varkappa \kappa} W_0 P - \frac{\delta \eta \rho \varepsilon}{\varkappa \upsilon \kappa} P \\ =& \frac{-\varpi}{U}\left(U - U_0\right)^2 - \frac{\delta \rho}{\varkappa \kappa}\frac{\beta}{W}\left(W - W_0\right)^2 + \left(\varrho U_0 - \frac{\delta \vartheta}{\varkappa} - \frac{\delta \rho}{\varkappa} W_0\right) V + \left(\frac{\delta \rho \nu}{\varkappa \kappa} W_0 - \frac{\delta \eta \rho \varepsilon}{\varkappa \upsilon \kappa}\right) P.\end{aligned}$$

Finally, we get

$$\frac{d\Lambda_0}{dt} = \frac{-\omega}{U}(U-U_0)^2 - \frac{\delta\rho}{\varkappa\kappa}\frac{\beta}{W}(W-W_0)^2 + \frac{\delta(\vartheta\beta+\rho\ell)}{\varkappa\beta}(R_2-1)V + \frac{\delta\eta\rho\varepsilon}{\varkappa\upsilon\kappa}(R_1-1)P.$$

Hence, $\frac{d\Lambda_0}{dt} \leq 0$ satisfies if $R_1 \leq 1$ and $R_2 \leq 1$. Further, $\frac{d\Lambda_0}{dt} = 0$ when $(U,W) = (U_0,W_0)$, $(R_2-1)V = 0$ and $(R_1-1)P = 0$. According to [53], T_0' is reached by the system's solutions. Thus, $(U,W) = (U_0,W_0)$,

$$(R_2-1)V = 0 \quad \text{and} \quad (R_1-1)P = 0. \tag{4.2}$$

are satisfied by any member in T_0'.

There are four cases at hand:

(I) $R_1 = 1$ and $R_2 = 1$. Then Eq. (2.1) gives

$$0 = \dot{U} = \xi - \omega U_0 - \varrho U_0 V \quad \Longrightarrow \quad V(t) = 0 \quad \text{for any } t. \tag{4.3}$$

From Eq. (2.3) we have

$$0 = \dot{V} = \varkappa Y \quad \Longrightarrow \quad Y(t) = 0 \quad \text{for any } t. \tag{4.4}$$

Eq. (2.4) implies that

$$0 = \dot{W} = \ell - \beta W_0 - \nu W_0 P \quad \Longrightarrow \quad P(t) = 0 \quad \text{for any } t. \tag{4.5}$$

Eq. (2.6) gives

$$0 = \dot{P} = \upsilon Z \quad \Longrightarrow \quad Z(t) = 0 \quad \text{for any } t. \tag{4.6}$$

Hence $T_0' = \{SS_0\}$.

(II) $R_1 < 1$ and $R_2 < 1$. Then from Eq. (4.2) we have $V = P = 0$ and Eqs. (4.4) and (4.6) imply $Y = Z = 0$. Consequently, $T_0' = \{SS_0\}$.

(III) $R_1 = 1$ and $R_2 < 1$. Then from Eq. (4.2) we get $V = 0$. Eqs. (4.4)-(4.6) imply $Y = P = Z = 0$. Thus $T_0' = \{SS_0\}$.

(IV) $R_1 < 1$ and $R_2 = 1$. Eq. (4.2) gives $P = 0$. Eqs. (4.3), (4.4) and (4.6) give, $V = Y = Z = 0$. Thus $T_0' = \{SS_0\}$.

By LaSalle's invariance principle [54], SS_0 is GAS. □

In order to demonstrate the instability of SS_0 if R_1 and/or R_2 are greater than 1.

To prove that if $R_1 > 1$ and/or $R_2 > 1$, then SS_0 is unstable, the Jacobian matrix $\mathcal{J} = \mathcal{J}(U,Y,V,W,Z,P)$ of model (2.1)-(2.6) is calculated as:

$$\mathcal{J} = \begin{pmatrix} -\omega-\varrho V & 0 & -\varrho U & 0 & 0 & 0 \\ \varrho V & -\delta & \varrho U & 0 & 0 & 0 \\ 0 & \varkappa & -\vartheta-\rho W & -\rho V & 0 & 0 \\ 0 & 0 & \kappa W & \kappa V-\beta-\nu P & 0 & -\nu W \\ 0 & 0 & 0 & \nu P & -\eta & \nu W \\ 0 & 0 & 0 & 0 & \upsilon & -\varepsilon \end{pmatrix}. \tag{4.7}$$

Consequently, at SS_0, the characteristic equation is provided by

$$\det(\mathcal{J}-\sigma I)=(\sigma+\omega)(\sigma+\beta)\Big(\tau_2\sigma^2+\tau_1\sigma+\tau_0\Big)\Big(\tilde{\tau}_2\sigma^2+\tilde{\tau}_1\sigma+\tilde{\tau}_0\Big)=0, \tag{4.8}$$

where, I is the identity matrix, σ the eigenvalues, and

$$\begin{aligned}
\tau_2 &= \beta,\\
\tau_1 &= \eta\beta+\varepsilon\beta,\\
\tau_0 &= \eta\varepsilon\beta-\ell\upsilon\nu=\eta\varepsilon\beta\,(1-R_1)\,,\\
\tilde{\tau}_2 &= \varpi\beta,\\
\tilde{\tau}_1 &= \varpi\rho\ell+\delta\varpi\beta+\vartheta\varpi\beta,\\
\tilde{\tau}_0 &= \delta\varpi(\vartheta\beta+\rho\ell)-\xi\varkappa\varrho\beta,\\
&= \delta\varpi(\vartheta\beta+\rho\ell)\,(1-R_2)\,.
\end{aligned}$$

$\tau_0<0$ and/or $\tilde{\tau}_0<0$, respectively, if $R_1>1$ and/or $R_2>1$. SS_0 is unstable as a result of Eq. (4.8) having a positive root. □

Theorem 4.2. *The KSHV mono-infection steady state SS_1 is GAS when $R_1>1$ and $R_3\leq 1$.*

Proof. Define $\Lambda_1(U,Y,V,W,Z,P)$ as:

$$\Lambda_1=U_1\mathcal{L}\Big(\frac{U}{U_1}\Big)+Y+\frac{\delta}{\varkappa}V+\frac{\delta\rho}{\varkappa\kappa}W_1\mathcal{L}\Big(\frac{W}{W_1}\Big)+\frac{\delta\rho}{\varkappa\kappa}Z_1\mathcal{L}\Big(\frac{Z}{Z_1}\Big)+\frac{\delta\eta\rho}{\varkappa\upsilon\kappa}P_1\mathcal{L}\Big(\frac{P}{P_1}\Big).$$

Clearly, $\Lambda_1(U,Y,V,W,Z,P)>0$ for any $U,Y,V,W,Z,P>0$ and $\Lambda_1(U_1,0,0,W_1,Z_1,P_1)=0$. Calculating $\frac{d\Lambda_1}{dt}$ as:

$$\frac{d\Lambda_1}{dt}=\Big(1-\frac{U_1}{U}\Big)\dot{U}+\dot{Y}+\frac{\delta}{\varkappa}\dot{V}+\frac{\delta\rho}{\varkappa\kappa}\Big(1-\frac{W_1}{W}\Big)\dot{W}+\frac{\delta\rho}{\varkappa\kappa}\Big(1-\frac{Z_1}{Z}\Big)\dot{Z}+\frac{\delta\eta\rho}{\varkappa\upsilon\kappa}\Big(1-\frac{P_1}{P}\Big)\dot{P}.$$

From Eqs. (2.1)-(2.6) we obtain

$$\begin{aligned}
\frac{d\Lambda_1}{dt}=&\Big(1-\frac{U_1}{U}\Big)(\xi-\omega U-\varrho UV)+(\varrho UV-\delta Y)+\frac{\delta}{\varkappa}\,(\varkappa Y-\vartheta V-\rho WV)\\
&+\frac{\delta\rho}{\varkappa\kappa}\Big(1-\frac{W_1}{W}\Big)(\ell+\kappa WV-\beta W-\nu PW)+\frac{\delta\rho}{\varkappa\kappa}\Big(1-\frac{Z_1}{Z}\Big)(\nu PW-\eta Z)\\
&+\frac{\delta\eta\rho}{\varkappa\upsilon\kappa}\Big(1-\frac{P_1}{P}\Big)(\upsilon Z-\varepsilon P)\,.
\end{aligned}$$

After collecting terms we get

$$\begin{aligned}
\frac{d\Lambda_1}{dt}=&\Big(1-\frac{U_1}{U}\Big)(\xi-\omega U)+\varrho U_1V-\frac{\delta\vartheta}{\varkappa}V+\frac{\delta\rho}{\varkappa\kappa}\Big(1-\frac{W_1}{W}\Big)(\ell-\beta W)-\frac{\delta\rho}{\varkappa}VW_1\\
&+\frac{\delta\rho\nu}{\varkappa\kappa}W_1P-\frac{\delta\rho\nu}{\varkappa\kappa}\frac{Z_1}{Z}WP+\frac{\delta\eta\rho}{\varkappa\kappa}Z_1-\frac{\delta\eta\rho}{\varkappa\kappa}\frac{P_1}{P}Z-\frac{\delta\eta\rho\varepsilon}{\varkappa\upsilon\kappa}P+\frac{\delta\eta\rho\varepsilon}{\varkappa\upsilon\kappa}P_1.
\end{aligned}$$

Using the following steady state conditions

$$\xi=\omega U_1,\quad \ell=\beta W_1+\nu W_1P_1,$$
$$\nu W_1P_1=\eta Z_1,\ \ \upsilon Z_1=\varepsilon P_1,$$

we get

$$\begin{aligned}\frac{d\Lambda_1}{dt} =&\frac{-\omega}{U}(U-U_1)^2-\frac{\delta\rho}{\varkappa\kappa}\frac{\beta}{W}(W-W_1)^2+\left(\varrho U_1-\frac{\delta\vartheta}{\varkappa}-\frac{\delta\rho}{\varkappa}W_1\right)V+\frac{\delta\rho\nu}{\varkappa\kappa}W_1P_1\\&-\frac{\delta\rho\nu}{\varkappa\kappa}\frac{W_1}{W}W_1P_1-\frac{\delta\rho\nu}{\varkappa\kappa}\frac{Z_1}{Z}WP+\frac{\delta\eta\rho}{\varkappa\kappa}Z_1-\frac{\delta\eta\rho}{\varkappa\kappa}\frac{P_1}{P}Z+\frac{\delta\eta\rho\varepsilon}{\varkappa\upsilon\kappa}P_1+\frac{\delta\rho}{\varkappa\kappa}\left(\nu W_1-\frac{\eta\varepsilon}{\upsilon}\right)P\\=&\frac{-\omega}{U}(U-U_1)^2-\frac{\delta\rho}{\varkappa\kappa}\frac{\beta}{W}(W-W_1)^2+\frac{\delta(\vartheta\upsilon\nu+\eta\varepsilon\rho)}{\varkappa\upsilon\nu}\left(\frac{\xi\varkappa\upsilon\nu\varrho}{\delta\omega(\vartheta\upsilon\nu+\eta\varepsilon\rho)}-1\right)V\\&+\frac{\delta\eta\rho}{\varkappa\kappa}Z_1-\frac{\delta\eta\rho}{\varkappa\kappa}\frac{W_1}{W}Z_1-\frac{\delta\eta\rho}{\varkappa\kappa}Z_1\frac{Z_1}{Z}\frac{W}{W_1}\frac{P}{P_1}+\frac{\delta\eta\rho}{\varkappa\kappa}Z_1-\frac{\delta\eta\rho}{\varkappa\kappa}Z_1\frac{P_1}{P}\frac{Z}{Z_1}+\frac{\delta\eta\rho}{\varkappa\kappa}Z_1\\=&\frac{-\omega}{U}(U-U_1)^2-\frac{\delta\rho}{\varkappa\kappa}\frac{\beta}{W}(W-W_1)^2+\frac{\delta(\vartheta\upsilon\nu+\eta\varepsilon\rho)}{\varkappa\upsilon\nu}(R_3-1)V\\&+\frac{\delta\eta\rho}{\varkappa\kappa}Z_1\left(3-\frac{W_1}{W}-\frac{Z_1WP}{ZW_1P_1}-\frac{P_1Z}{PZ_1}\right).\end{aligned}$$

Thus, if $R_1 > 1$, $R_3 \leq 1$ and by using inequality (4.1), we conclude that $\frac{d\Lambda_1}{dt} \leq 0$ for any $U, Y, V, W, Z, P > 0$. Also, we have $\frac{d\Lambda_1}{dt} = 0$ if $(U, W, Z, P) = (U_1, W_1, Z_1, P_1)$ and $(R_3 - 1)V = 0$. T_1' is reached by the model's solutions. In T_1' we have $(U, W, Z, P) = (U_1, W_1, Z_1, P_1)$ and

$$(R_3 - 1)V = 0. \tag{4.9}$$

Two cases are at hand:

(I) $R_3 = 1$, then Eq. (2.1) provides

$$0 = \dot{U} = \xi - \omega U_1 - \varrho U_1 V \quad \Longrightarrow \quad V(t) = 0 \quad \text{for any } t. \tag{4.10}$$

Moreover, Eq. (2.3) gives

$$0 = \dot{V} = \varkappa Y \quad \Longrightarrow \quad Y(t) = 0 \quad \text{for any } t. \tag{4.11}$$

The $T_1' = \{SS_1\}$.

(II) $R_3 < 1$, thus Eq. (4.9) gives $V = 0$ and Eq. (4.11) yields $Y = 0$ and thus $T_1' = \{SS_1\}$.

Thus, by LaSalle's invariance principle, SS_1 is GAS. □

Theorem 4.3. *The HIV-1 mono-infection steady state SS_2 is GAS when $R_2 > 1$ and $R_4 \leq 1$.*

Proof. Let us formulate a function $\Lambda_2(U, Y, V, W, Z, P)$ as:

$$\Lambda_2 = U_2\mathcal{L}\left(\frac{U}{U_2}\right)+Y_2\mathcal{L}\left(\frac{Y}{Y_2}\right)+\frac{\delta}{\varkappa}V_2\mathcal{L}\left(\frac{V}{V_2}\right)+\frac{\delta\rho}{\varkappa\kappa}W_2\mathcal{L}\left(\frac{W}{W_2}\right)+\frac{\delta\rho}{\varkappa\kappa}Z+\frac{\delta\eta\rho}{\varkappa\upsilon\kappa}P.$$

Clearly, $\Lambda_2(U, Y, V, W, Z, P) > 0$ for any $U, Y, V, W, Z, P > 0$ and $\Lambda_2(U_2, Y_2, V_2, W_2, 0, 0) = 0$. Calculating $\frac{d\Lambda_2}{dt}$ as:

$$\frac{d\Lambda_2}{dt} = \left(1-\frac{U_2}{U}\right)\dot{U}+\left(1-\frac{Y_2}{Y}\right)\dot{Y}+\frac{\delta}{\varkappa}\left(1-\frac{V_2}{V}\right)\dot{V}+\frac{\delta\rho}{\varkappa\kappa}\left(1-\frac{W_2}{W}\right)\dot{W}+\frac{\delta\rho}{\varkappa\kappa}\dot{Z}+\frac{\delta\eta\rho}{\varkappa\upsilon\kappa}\dot{P}.$$

From Eqs. (2.1)-(2.6) we obtain

$$\frac{d\Lambda_2}{dt} =\left(1-\frac{U_2}{U}\right)(\xi-\omega U-\varrho UV)+\left(1-\frac{Y_2}{Y}\right)(\varrho UV-\delta Y)+\frac{\delta}{\varkappa}\left(1-\frac{V_2}{V}\right)(\varkappa Y-\vartheta V-\rho WV)$$

$$+\frac{\delta\rho}{\varkappa\kappa}\left(1-\frac{W_2}{W}\right)(\ell+\kappa WV-\beta W-\nu PW)+\frac{\delta\rho}{\varkappa\kappa}(\nu PW-\eta Z)+\frac{\delta\eta\rho}{\varkappa\upsilon\kappa}(\upsilon Z-\varepsilon P).$$

Collecting terms we get

$$\begin{aligned}\frac{d\Lambda_2}{dt}=&\left(1-\frac{U_2}{U}\right)(\xi-\omega U)+\varrho U_2V-\varrho UV\frac{Y_2}{Y}+\delta Y_2-\delta Y\frac{V_2}{V}-\frac{\delta\vartheta}{\varkappa}V+\frac{\delta\vartheta}{\varkappa}V_2+\frac{\delta\rho}{\varkappa}WV_2\\&+\frac{\delta\rho}{\varkappa\kappa}\left(1-\frac{W_2}{W}\right)(\ell-\beta W)-\frac{\delta\rho}{\varkappa}VW_2+\frac{\delta\rho\nu}{\varkappa\kappa}W_2P-\frac{\delta\eta\rho\varepsilon}{\varkappa\upsilon\kappa}P.\end{aligned}$$

Applying the steady state conditions

$$\xi=\omega U_2+\varrho U_2V_2,\qquad \varrho U_2V_2=\delta Y_2,$$
$$\varkappa Y_2=\vartheta V_2+\rho W_2V_2,\qquad \ell=-\kappa W_2V_2+\beta W_2,$$

we obtain

$$\begin{aligned}\frac{d\Lambda_2}{dt}=&\frac{-\omega}{U}(U-U_2)^2+\left(1-\frac{U_2}{U}\right)\varrho U_2V_2-\frac{\delta\rho}{\varkappa\kappa}\frac{\beta}{W}(W-W_2)^2-\frac{\delta\rho}{\varkappa}\left(1-\frac{W_2}{W}\right)V_2W_2+\varrho U_2V\\&-\varrho UV\frac{Y_2}{Y}+\delta Y_2-\delta Y\frac{V_2}{V}-\frac{\delta\vartheta}{\varkappa}V+\frac{\delta\vartheta}{\varkappa}V_2+\frac{\delta\rho}{\varkappa}WV_2-\frac{\delta\rho}{\varkappa}VW_2+\frac{\delta\rho\nu}{\varkappa\kappa}W_2P-\frac{\delta\eta\rho\varepsilon}{\varkappa\upsilon\kappa}P\\=&\frac{-\omega}{U}(U-U_2)^2-\frac{\delta\rho}{\varkappa\kappa}\frac{\beta}{W}(W-W_2)^2+\left(\varrho U_2-\frac{\delta\vartheta}{\varkappa}-\frac{\delta\rho}{\varkappa}W_2\right)V+\frac{\delta\rho}{\varkappa\kappa}\left(\nu W_2-\frac{\eta\varepsilon}{\upsilon}\right)P\\&+\varrho U_2V_2-\varrho U_2V_2\frac{U_2}{U}-\frac{\delta\rho}{\varkappa}V_2W_2+\frac{\delta\rho}{\varkappa}V_2W_2\frac{W_2}{W}-\varrho UV\frac{Y_2}{Y}+\delta Y_2-\delta Y\frac{V_2}{V}+\frac{\delta\vartheta}{\varkappa}V_2\\&+\frac{\delta\rho}{\varkappa}WV_2+\frac{\delta\rho}{\varkappa}V_2W_2-\frac{\delta\rho}{\varkappa}V_2W_2\\=&\frac{-\omega}{U}(U-U_2)^2-\frac{\delta\rho}{\varkappa\kappa}\frac{\beta}{W}(W-W_2)^2+\left(\varrho U_2-\frac{\delta\vartheta}{\varkappa}-\frac{\delta\rho}{\varkappa}W_2\right)V+\frac{\delta\rho}{\varkappa\kappa}\left(\nu W_2-\frac{\eta\varepsilon}{\upsilon}\right)P\\&+\delta Y_2\left(3-\frac{U_2}{U}-\frac{U}{U_2}\frac{V}{V_2}\frac{Y_2}{Y}-\frac{Y}{Y_2}\frac{V_2}{V}\right)-\frac{\delta\rho}{\varkappa}V_2W_2\left(2-\frac{W_2}{W}-\frac{W}{W_2}\right)\\=&\frac{-\omega}{U}(U-U_2)^2-\frac{\delta\rho}{\varkappa\kappa}\frac{\ell}{WW_2}(W-W_2)^2+\frac{\delta\rho\nu}{\varkappa\kappa}(W_2-W_3)P+\delta Y_2\left(3-\frac{U_2}{U}-\frac{U}{U_2}\frac{V}{V_2}\frac{Y_2}{Y}-\frac{Y}{Y_2}\frac{V_2}{V}\right).\end{aligned}$$

Now we show that if $R_4\le 1$, then $W_2\le W_3$. In case $R_4\le 1$, then co-infection steady state SS_3 does not exist since $Z_3\le 0$ and $P_3\le 0$. Thus,

$$\dot{Z}=\nu PW-\eta Z\le 0,$$
$$\dot{P}=\upsilon Z-\varepsilon P\le 0.$$

We need to find a value $\bar{W}$ where $0<W(t)\le\bar{W}$ such that $\dot{Z}(t)\le 0$ and $\dot{P}\le 0$. We have

$$\dot{Z}+\frac{\eta}{\upsilon}\dot{P}=\nu PW-\frac{\eta\varepsilon}{\upsilon}P=\nu\left(W-\frac{\eta\varepsilon}{\nu\upsilon}\right)P\le 0\qquad\text{for any } Z,P>0.$$

This occurs when $W_2\le\bar{W}=\frac{\eta\varepsilon}{\nu\upsilon}=W_3$. Inequality (4.1) yields $\frac{d\Lambda_2}{dt}\le 0$, where equality holds when $(U,Y,V,W)=(U_2,Y_2,V_2,W_2)$ and $(W_2-W_3)P=0$. The model's solutions reach T_2' which has elements with $(U,Y,V,W)=(U_2,Y_2,V_2,W_2)$ and

$$(W_2-W_3)P=0,\tag{4.12}$$

and we have two cases:

(I) $W_2 = W_3$. From Eq. (2.4) we have

$$0 = \dot{W} = \ell + \kappa W_2 V_2 - \beta W_2 - \nu P W_2 \quad \Longrightarrow \quad P(t) = 0 \quad \text{for any } t.$$

Eq. (2.6) gives

$$0 = \dot{P} = \upsilon Z \quad \Longrightarrow \quad Z(t) = 0 \quad \text{for any } t. \tag{4.13}$$

Hence $T_2' = \{SS_2\}$.

(II) $W_2 < W_3$. Eq. (4.12) yields $P = 0$ and Eq. (4.13) gives $Z = 0$. Thus $T_2' = \{SS_2\}$.

Consequently, by LaSalle's invariance principle, SS_2 is GAS. □

Theorem 4.4. *The KSHV/HIV-1 co-infection steady state SS_3 is GAS when $R_4 > 1$ and $1 < R_3 \leq 1 + \frac{\beta\varrho}{\omega\kappa}$.*

Proof. Define $\Lambda_3(U, Y, V, W, Z, P)$ as:

$$\Lambda_3 = U_3 \mathcal{L}\left(\frac{U}{U_3}\right) + Y_3 \mathcal{L}\left(\frac{Y}{Y_3}\right) + \frac{\delta}{\varkappa} V_3 \mathcal{L}\left(\frac{V}{V_3}\right) + \frac{\delta\rho}{\varkappa\kappa} W_3 \mathcal{L}\left(\frac{W}{W_3}\right) + \frac{\delta\rho}{\varkappa\kappa} Z_3 \mathcal{L}\left(\frac{Z}{Z_3}\right) + \frac{\delta\eta\rho}{\varkappa\upsilon\kappa} P_3 \mathcal{L}\left(\frac{P}{P_3}\right).$$

Calculating $\frac{d\Lambda_3}{dt}$ as:

$$\frac{d\Lambda_3}{dt} = \left(1 - \frac{U_3}{U}\right)\dot{U} + \left(1 - \frac{Y_3}{Y}\right)\dot{Y} + \frac{\delta}{\varkappa}\left(1 - \frac{V_3}{V}\right)\dot{V} + \frac{\delta\rho}{\varkappa\kappa}\left(1 - \frac{W_3}{W}\right)\dot{W} + \frac{\delta\rho}{\varkappa\kappa}\left(1 - \frac{Z_3}{Z}\right)\dot{Z} + \frac{\delta\eta\rho}{\varkappa\upsilon\kappa}\left(1 - \frac{P_3}{P}\right)\dot{P}.$$

Using equation of model (2.1)-(2.6), we obtain

$$\begin{aligned}\frac{d\Lambda_3}{dt} =& \left(1 - \frac{U_3}{U}\right)(\xi - \omega U - \varrho U V) + \left(1 - \frac{Y_3}{Y}\right)(\varrho U V - \delta Y) + \frac{\delta}{\varkappa}\left(1 - \frac{V_3}{V}\right)(\varkappa Y - \vartheta V - \rho V W) \\ &+ \frac{\delta\rho}{\varkappa\kappa}\left(1 - \frac{W_3}{W}\right)(\ell + \kappa W V - \beta W - \nu P W) + \frac{\delta\rho}{\varkappa\kappa}\left(1 - \frac{Z_3}{Z}\right)(\nu P W - \eta Z) \\ &+ \frac{\delta\eta\rho}{\varkappa\upsilon\kappa}\left(1 - \frac{P_3}{P}\right)(\upsilon Z - \varepsilon P).\end{aligned}$$

Collecting terms as:

$$\begin{aligned}\frac{d\Lambda_3}{dt} =& \left(1 - \frac{U_3}{U}\right)(\xi - \omega U) + \varrho U_3 V - \varrho U V \frac{Y_3}{Y} + \delta Y_3 - \delta Y \frac{V_3}{V} - \frac{\delta\vartheta}{\varkappa} V + \frac{\delta\vartheta}{\varkappa} V_3 + \frac{\delta\rho}{\varkappa} W V_3 \\ &+ \frac{\delta\rho}{\varkappa\kappa}\left(1 - \frac{W_3}{W}\right)(\ell - \beta W) - \frac{\delta\rho}{\varkappa} V W_3 + \frac{\delta\rho\nu}{\varkappa\kappa} W_3 P - \frac{\delta\rho\nu}{\varkappa\kappa} W P \frac{Z_3}{Z} + \frac{\delta\eta\rho}{\varkappa\kappa} Z_3 - \frac{\delta\eta\rho}{\varkappa\kappa} Z \frac{P_3}{P} \\ &- \frac{\delta\eta\rho\varepsilon}{\varkappa\upsilon\kappa} P + \frac{\delta\eta\rho\varepsilon}{\varkappa\upsilon\kappa} P_3.\end{aligned}$$

Using the steady state conditions

$$\begin{aligned}\xi = \omega U_3 + \varrho U_3 V_3, \quad \varrho U_3 V_3 = \delta Y_3, \\ \varkappa Y_3 = \vartheta V_3 + \rho V_3 W_3, \quad \ell = -\kappa W_3 V_3 + \beta W_3 + \nu W_3 P_3, \\ \nu P_3 W_3 = \eta Z_3, \quad \upsilon Z_3 = \varepsilon P_3,\end{aligned}$$

we get

$$\frac{d\Lambda_3}{dt} = \frac{-\omega}{U}(U - U_3)^2 + \left(1 - \frac{U_3}{U}\right)\varrho U_3 V_3 - \frac{\delta\rho}{\varkappa\kappa}\frac{\beta}{W}(W - W_3)^2 - \frac{\delta\rho}{\varkappa}\left(1 - \frac{W_3}{W}\right) V_3 W_3$$

$$
\begin{aligned}
&+\frac{\delta\rho\nu}{\varkappa\kappa}\left(1-\frac{W_3}{W}\right)W_3P_3+\varrho U_3V-\varrho UV\frac{Y_3}{Y}+\delta Y_3-\delta Y\frac{V_3}{V}-\frac{\delta\vartheta}{\varkappa}V+\frac{\delta\vartheta}{\varkappa}V_3+\frac{\delta\rho}{\varkappa}WV_3\\
&-\frac{\delta\rho}{\varkappa}VW_3+\frac{\delta\rho\nu}{\varkappa\kappa}W_3P-\frac{\delta\rho\nu}{\varkappa\kappa}WP\frac{Z_3}{Z}+\frac{\delta\eta\rho}{\varkappa\kappa}Z_3-\frac{\delta\eta\rho}{\varkappa\kappa}Z\frac{P_3}{P}-\frac{\delta\eta\rho\varepsilon}{\varkappa\upsilon\kappa}P+\frac{\delta\eta\rho\varepsilon}{\varkappa\upsilon\kappa}P_3\\
=&\frac{-\omega}{U}\left(U-U_3\right)^2-\frac{\delta\rho}{\varkappa\kappa}\frac{\beta}{W}\left(W-W_3\right)^2+\varrho U_3V_3-\varrho U_3V_3\frac{U_3}{U}-\frac{\delta\rho}{\varkappa}V_3W_3+\frac{\delta\rho}{\varkappa}\frac{W_3}{W}V_3W_3\\
&+\frac{\delta\rho\nu}{\varkappa\kappa}W_3P_3-\frac{\delta\rho\nu}{\varkappa\kappa}\frac{W_3}{W}W_3P_3+\varrho U_3V-\varrho UV\frac{Y_3}{Y}+\delta Y_3-\delta Y\frac{V_3}{V}-\frac{\delta\vartheta}{\varkappa}V+\frac{\delta\vartheta}{\varkappa}V_3\\
&+\frac{\delta\rho}{\varkappa}WV_3-\frac{\delta\rho}{\varkappa}VW_3+\frac{\delta\rho\nu}{\varkappa\kappa}W_3P-\frac{\delta\rho\nu}{\varkappa\kappa}WP\frac{Z_3}{Z}+\frac{\delta\eta\rho}{\varkappa\kappa}Z_3-\frac{\delta\eta\rho}{\varkappa\kappa}Z\frac{P_3}{P}-\frac{\delta\eta\rho\varepsilon}{\varkappa\upsilon\kappa}P\\
&+\frac{\delta\eta\rho\varepsilon}{\varkappa\upsilon\kappa}P_3+\frac{\delta\rho}{\varkappa}V_3W_3-\frac{\delta\rho}{\varkappa}V_3W_3.
\end{aligned}
$$

It follows that

$$
\begin{aligned}
\frac{d\Lambda_3}{dt}=&\frac{-\omega}{U}\left(U-U_3\right)^2-\frac{\delta\rho}{\varkappa\kappa}\frac{\beta}{W}\left(W-W_3\right)^2+\left(\varrho U_3-\frac{\delta\vartheta}{\varkappa}-\frac{\delta\rho}{\varkappa}W_3\right)V+\frac{\delta\rho}{\varkappa\kappa}\left(\nu W_3-\frac{\eta\varepsilon}{\upsilon}\right)P\\
&+\delta Y_3\left(3-\frac{U_3}{U}-\frac{UVY_3}{U_3V_3Y}-\frac{YV_3}{Y_3V}\right)-\frac{\delta\rho}{\varkappa}V_3W_3\left(2-\frac{W_3}{W}-\frac{W}{W_3}\right)\\
&+\frac{\delta\rho\nu}{\varkappa\kappa}W_3P_3\left(3-\frac{W_3}{W}-\frac{WZ_3P}{W_3ZP_3}-\frac{ZP_3}{Z_3P}\right)\\
=&\frac{-\omega}{U}\left(U-U_3\right)^2-\frac{\delta\rho}{\varkappa\kappa}\frac{\beta}{W}\left(W-W_3\right)^2+\delta Y_3\left(3-\frac{U_3}{U}-\frac{UVY_3}{U_3V_3Y}-\frac{YV_3}{Y_3V}\right)\\
&-\frac{\delta\rho}{\varkappa}V_3W_3\left(2-\frac{W_3}{W}-\frac{W}{W_3}\right)+\frac{\delta\rho\nu}{\varkappa\kappa}W_3P_3\left(3-\frac{W_3}{W}-\frac{WZ_3P}{W_3ZP_3}-\frac{ZP_3}{Z_3P}\right)\\
=&\frac{-\omega}{U}\left(U-U_3\right)^2-\frac{\delta\rho}{\varkappa\kappa}\frac{\beta}{W}\left(W-W_3\right)^2+\delta Y_3\left(3-\frac{U_3}{U}-\frac{UVY_3}{U_3V_3Y}-\frac{YV_3}{Y_3V}\right)\\
&+\frac{\delta\rho}{\varkappa}\frac{V_3}{W}\left(W-W_3\right)^2+\frac{\delta\rho\nu}{\varkappa\kappa}W_3P_3\left(3-\frac{W_3}{W}-\frac{WZ_3P}{W_3ZP_3}-\frac{ZP_3}{Z_3P}\right).
\end{aligned}
$$

Finally, we get

$$
\begin{aligned}
\frac{d\Lambda_3}{dt}=&\frac{-\omega}{U}\left(U-U_3\right)^2+\frac{\delta\rho\omega}{\varkappa\varrho}\frac{1}{W}\left(W-W_3\right)^2\left(R_3-1-\frac{\beta\varrho}{\omega\kappa}\right)+\delta Y_3\left(3-\frac{U_3}{U}-\frac{UVY_3}{U_3V_3Y}-\frac{YV_3}{Y_3V}\right)\\
&+\frac{\delta\rho\nu}{\varkappa\kappa}W_3P_3\left(3-\frac{W_3}{W}-\frac{WZ_3P}{W_3ZP_3}-\frac{ZP_3}{Z_3P}\right).
\end{aligned}
$$

Thus, if $1<R_3\leq 1+\frac{\beta\varrho}{\omega\kappa}$ and by using inequality (4.1), we conclude that $\frac{d\Lambda_3}{dt}\leq 0$ for any $U,Y,V,W,Z,P>0$. In addition, $\frac{d\Lambda_3}{dt}=0$ if $(U,Y,V,W,Z,P)=(U_3,Y_3,V_3,W_3,Z_3,P_3)$. Solutions of model (2.1)-(2.6) reach to T_3' where $(U,Y,V,W,Z,P)=(U_3,Y_3,V_3,W_3,Z_3,P_3)$. Hence, $T_3'=\{SS_3\}$ and SS_3 is GAS using LaSalle's invariance principle. □

Table 2 provides an overview of the global stability conditions for each of the model's steady states.

TABLE 2. Conditions for an equilibrium's existence and stability.

Steady state	Existence condition	Stability condition
$SS_0 = (U_0, 0, 0, W_0, 0, 0)$	-	$R_1 \leq 1$ and $R_2 \leq 1$
$SS_1 = (U_1, 0, 0, W_1, Z_1, P_1)$	$R_1 > 1$	$R_1 > 1$ and $R_3 \leq 1$
$SS_2 = (U_2, Y_2, V_2, W_2, 0, 0)$	$R_2 > 1$	$R_2 > 1$ and $R_4 \leq 1$
$SS_3 = (U_3, Y_3, V_3, W_3, Z_3, P_3)$	$R_3 > 1, R_4 > 1$	$R_4 > 1$ and $1 < R_3 \leq 1 + \frac{\beta\varrho}{\omega\kappa}$

5. NUMERICAL SIMULATIONS

5.1. **Numerical simulations for system (2.1)-(2.6).** In this section, numerical simulations are provided to visualize the analytical results that obtain in previous section by using the parameter's values that provided in Table 1. The initial conditions of model (2.1)-(2.6) are taken as:

$$\textbf{Initial.1} : U(0) = 200, Y(0) = 20, V(0) = 25, W(0) = 200, Z(0) = 150, P(0) = 300.$$

$$\textbf{Initial.2} : U(0) = 400, Y(0) = 15, V(0) = 20, W(0) = 300, Z(0) = 100, P(0) = 200.$$

$$\textbf{Initial.3} : U(0) = 600, Y(0) = 10, V(0) = 15, W(0) = 400, Z(0) = 50, P(0) = 100.$$

The values the parameters ϱ and ν are selected and leading to the following circumstances:

Circumstance-1: $\varrho = 0.0001$ and $\nu = 0.0005$. For these values of parameters, we have $R_1 = 0.53 < 1$ and $R_2 = 0.42 < 1$. Starting with the three initials the trajectories lead to the steady state $SS_0 = (1000, 0, 0, 200, 0, 0)$, as Figure 2 illustrates. This demonstrates that, according to Theorem 1, SS_0 is GAS. This will result in the clearance of both KSHV and HIV-1. Making $R_1 \leq 1$ and $R_2 \leq 1$ may be achieved if there are efficient drug therapies for both KSHV and HIV-1.

Circumstance-2: $\varrho = 0.0001$ and $\nu = 0.002$. This yields $R_1 = 2.1 > 1$ and $R_3 = 0.8 < 1$. The findings in Figure 3 demonstrate how the solutions approach the steady state, $SS_1 = (1000, 0, 0, 94.05, 77.05, 135.18)$. Consequently, Theorem 2 and the numerical findings match. This instance illustrates what happens when a person has KSHV infection but not HIV-1 infection. It is evident that KSHV infection has resulted in decreased B cell numbers, while $CD4^+$T cell concentrations are still within normal limits.

Circumstance-3: $\varrho = 0.001$ and $\nu = 0.0001$. Then, we calculate $R_2 = 4.2 > 1$ and $R_4 = 0.22 < 1$. It is evident that the requirements listed in Table 2 are met. Theorem 3 is supported by Figure 4, which shows that the solutions converge to the steady state $SS_2 = (451.53, 13.71, 12.14, 404.96, 0, 0)$. This instance illustrates what happens when a person has HIV-1 infection but not KSHV infection. It is evident that HIV-1 infection has resulted in decreased $CD4^+$T cell numbers. The presence of HIV-1 stimulates the B cells and increases their concentration.

Circumstance-4: $\varrho = 0.001$ and $\nu = 0.0006$. These data provide $R_4 = 1.3 > 1$, $R_3 = 2.8 > 1$ and $R_3 < 1 + \frac{\beta\varrho}{\omega\kappa} = 3.4$. Figure 5 show that $SS_3 = (355.26, 16.12, 18.15, 313.5, 89.86, 157.65)$

exist, and is GAS as we have proved in Theorem 4. Here, KSHV and HIV-1 are co-infected in a human. The possibility of KSHV elimination is reduced due to a drop in the quantity of both $CD4^+$ T cells and B cells. Furthermore, the patient's immune system may be deteriorating, which might lead to a rise in the manifestation of illness symptoms. This might raise the likelihood that the patient would pass away.

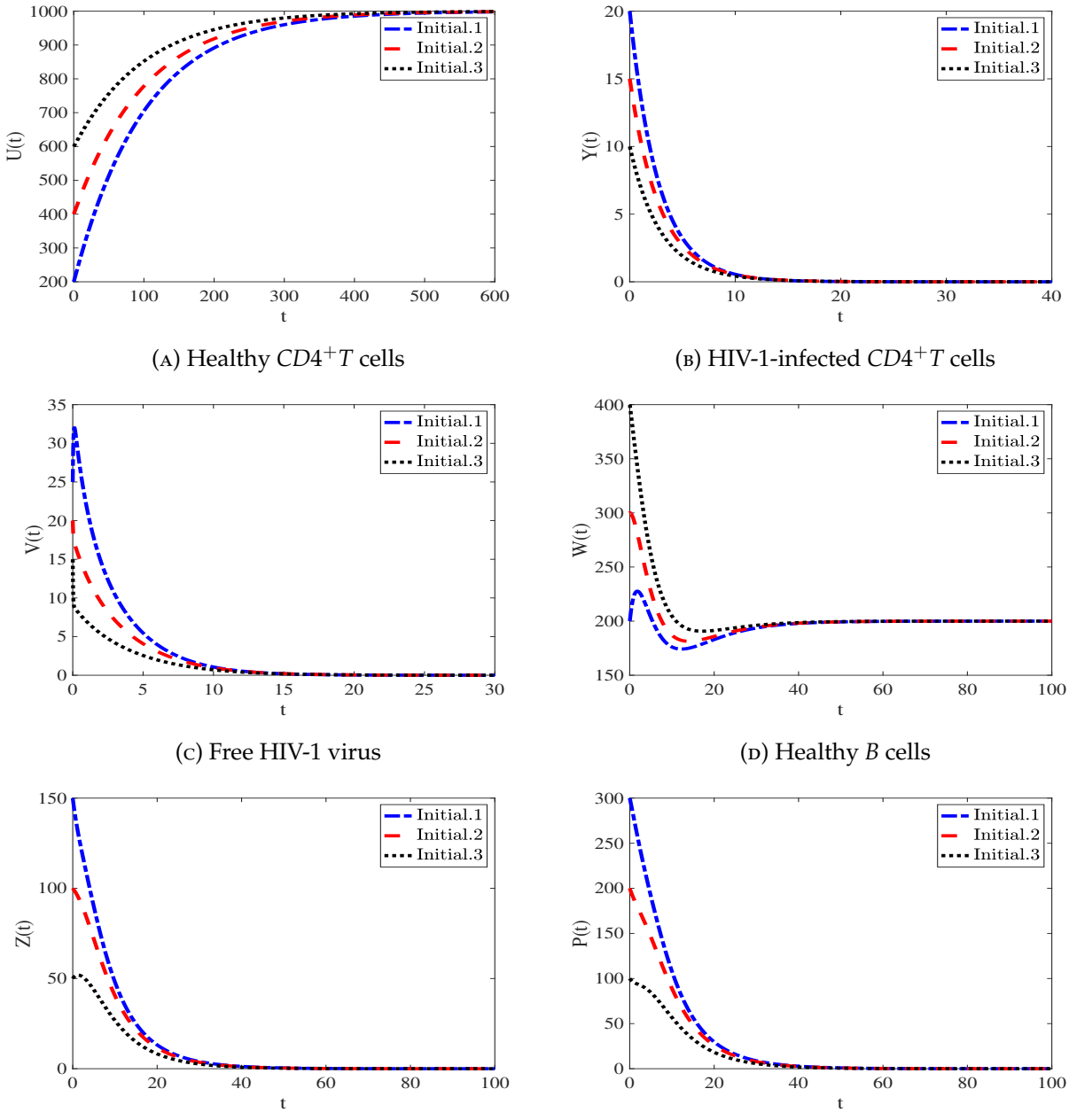

(A) Healthy $CD4^+T$ cells

(B) HIV-1-infected $CD4^+T$ cells

(C) Free HIV-1 virus

(D) Healthy B cells

(E) KSHV-infected B cells

(F) Free KSHV virus

FIGURE 2. Solutions of system (2.1)-(2.6) with three different initials reach healthy steady state $SS_0 = (1000, 0, 0, 200, 0, 0)$.

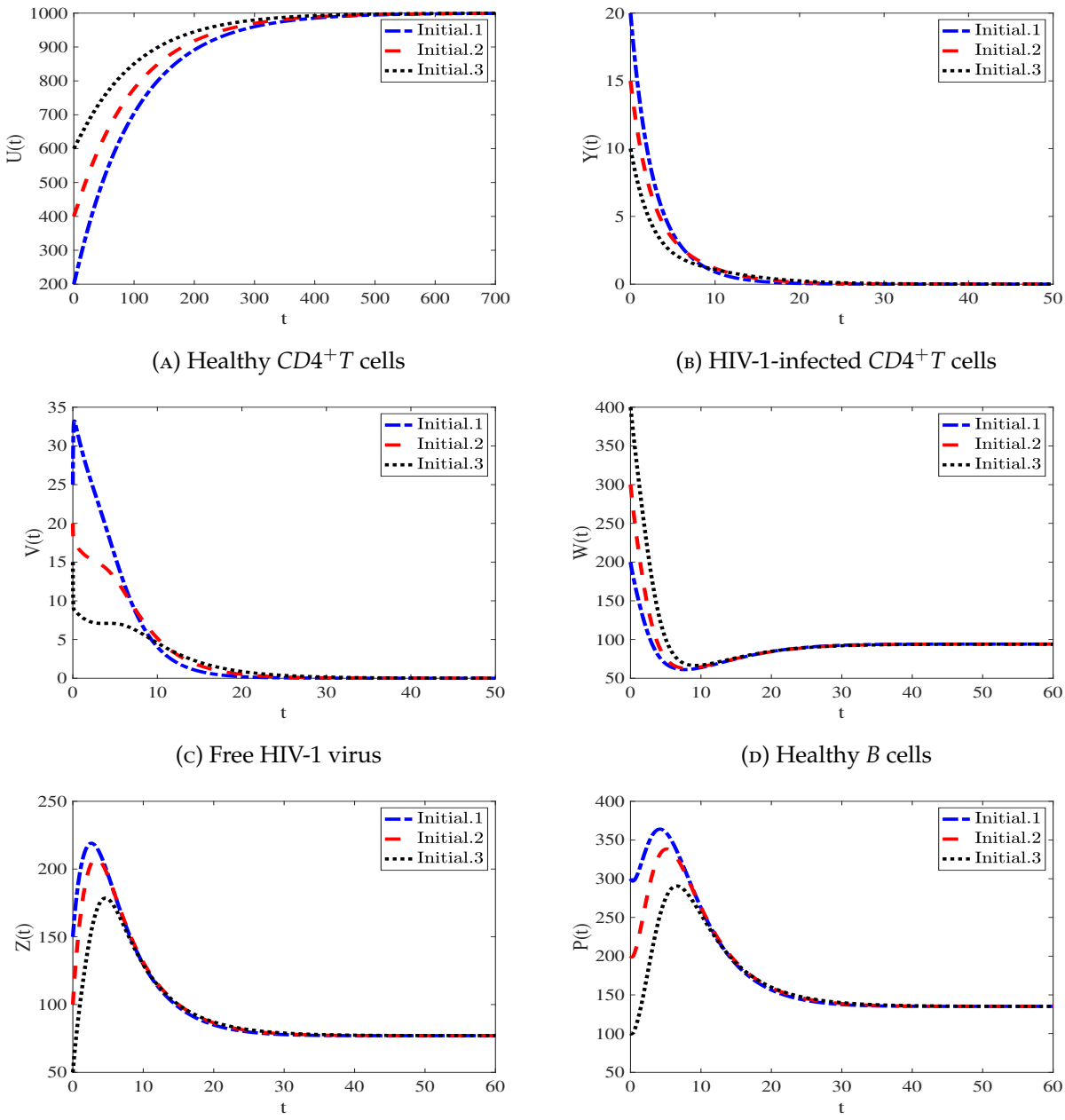

(A) Healthy $CD4^+T$ cells

(B) HIV-1-infected $CD4^+T$ cells

(C) Free HIV-1 virus

(D) Healthy B cells

(E) KSHV-infected B cells

(F) Free KSHV virus

FIGURE 3. Solutions of system (2.1)-(2.6) with three different initials reach the KSHV mono-infection steady state $SS_1 = (1000, 0, 0, 94.05, 77.05, 135.18)$.

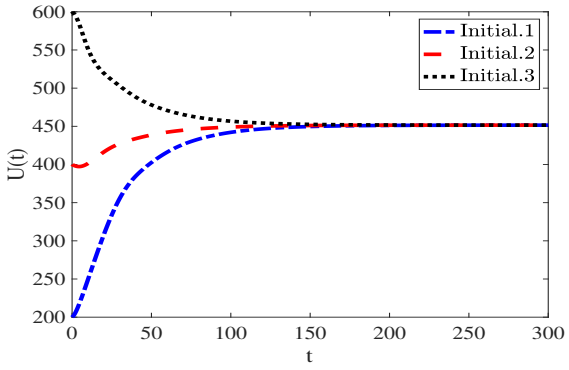

(A) Healthy $CD4^+T$ cells

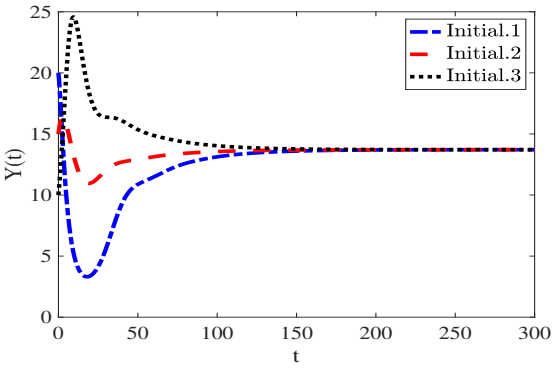

(B) HIV-1-infected $CD4^+T$ cells

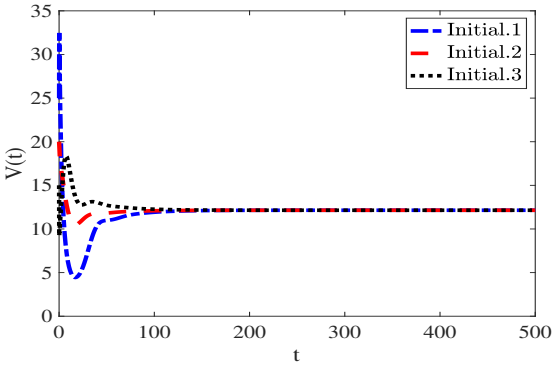

(C) Free HIV-1 virus

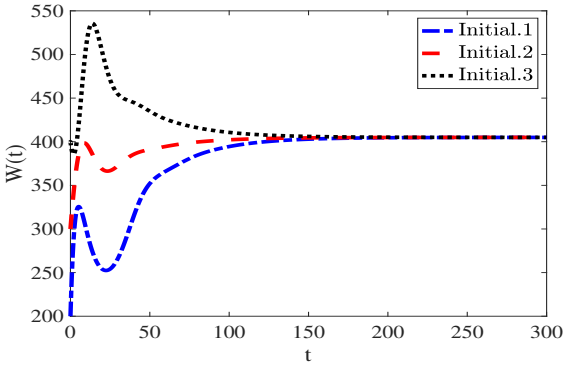

(D) Healthy B cells

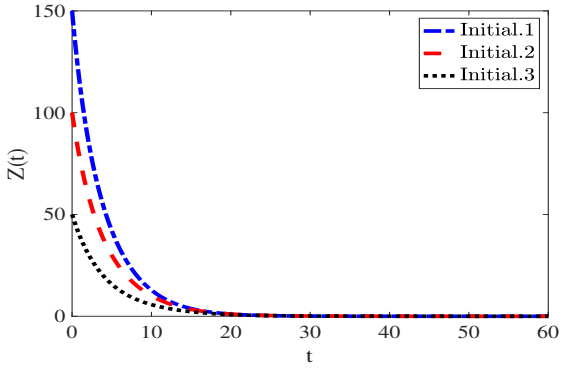

(E) KSHV-infected B cells

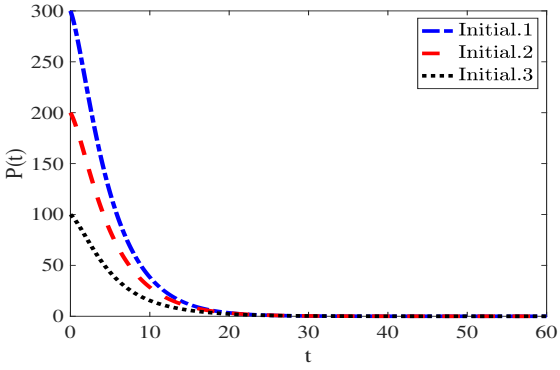

(F) Free KSHV virus

FIGURE 4. Solutions of system (2.1)-(2.6) with three different initials reach the HIV-1 mono-infection steady state $SS_2 = (451.53, 13.71, 12.14, 404.96, 0, 0)$.

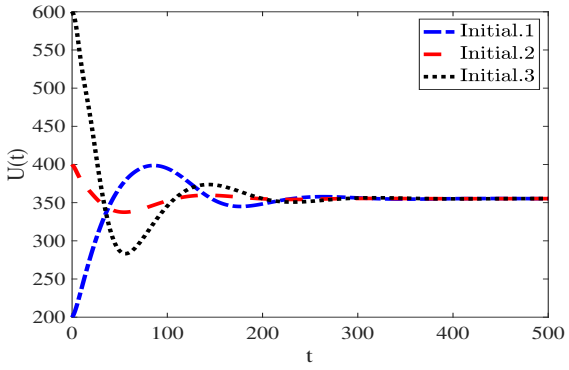

(A) Healthy $CD4^+T$ cells

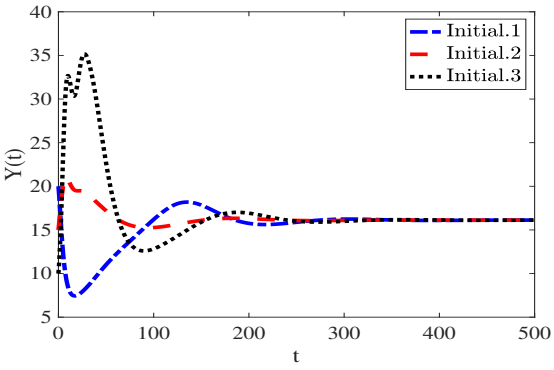

(B) HIV-1-infected $CD4^+T$ cells

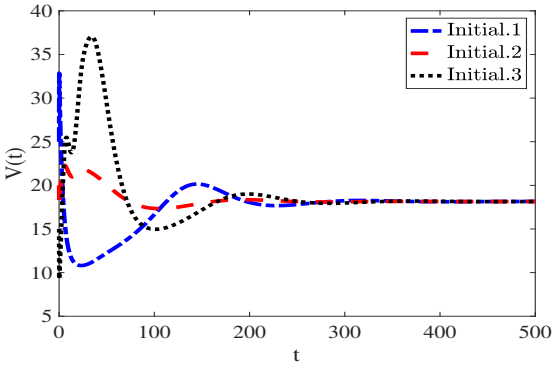

(C) Free HIV-1 virus

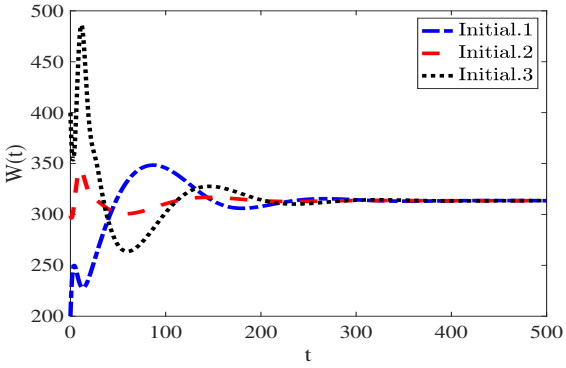

(D) Healthy B cells

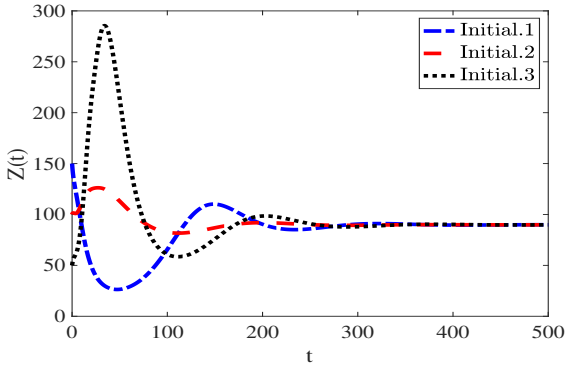

(E) KSHV-infected B cells

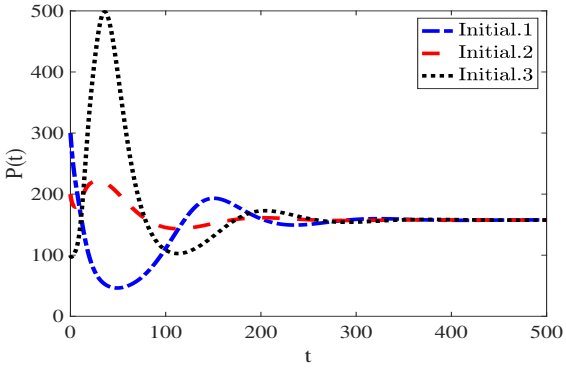

(F) Free KSHV virus

FIGURE 5. Solutions of system (2.1)-(2.6) with three different initials reach the KSHV/HIV-1 co-infection steady state $SS_3 = (355.26, 16.12, 18.15, 313.5, 89.86, 157.65)$.

For further confirmation, a study of local stability for any steady state are provided. The jacobian matrix $\mathcal{J} = \mathcal{J}(U, Y, V, W, Z, P)$ of model (2.1)-(2.6) is computed in (4.7). For each steady state, we compute the eigenvalues $\lambda_i, i = 1, \cdots, 6$ of $\mathcal{J}$. An steady state point is locally stable if the eigenvalues satisfy $\mathrm{Re}(\lambda_i) < 0$ for all $i = 1, 2, \cdots, 6$. By computing all the nonnegative steady state and using the parameter's value that written in Circumstance 1-4, we deduce the eigenvalues corresponding to all steady states. Table 3 outlined all positive steady states and the real part of the eigenvalues.

TABLE 3. Local stability of steady states.

Circumstance	Equilibrium	$\mathrm{Re}(\lambda_i) < 0, i = 1, \cdots, 6$	Stability
1	$SS_0 = (1000, 0, 0, 200, 0, 0)$	$(-22.57, -0.79, -0.24, -0.23, -0.11, -0.01)$	stable
2	$SS_0 = (1000, 0, 0, 200, 0, 0)$	$(-22.57, -1.1, -0.24, -0.23, 0.19, -0.01)$	unstable
	$SS_1 = (1000, 0, 0, 94.05, 77.05, 135.18)$	$(-12.13, -1., -0.4, -0.2, -0.2, -0.01)$	stable
3	$SS_0 = (1000, 0, 0, 200, 0, 0)$	$(-24, 1.2, -0.64, -0.26, -0.24, -0.01)$	unstable
	$SS_2 = (451.53, 13.71, 12.14, 404.96, 0, 0)$	$(-43.18, -0.68, -0.11, -0.11, -0.22, -0.033)$	stable
4	$SS_0 = (1000, 0, 0, 200, 0, 0)$	$(-24, 1.2, -0.82, -0.24, -0.083, -0.01)$	unstable
	$SS_2 = (451.53, 13.71, 12.15, 404.96, 0, 0)$	$(-43.18, -0.96, -0.11, -0.11, 0.057, -0.033)$	unstable
	$SS_3 = (355.26, 16.12, 18.15, 313.5, 89.86, 157.65)$	$(-33.98, -0.93, -0.14, -0.14, -0.016, -0.016)$	stable

5.2. **Sensitivity Analysis.** Sensitivity analysis is a crucial method in biological systems that helps to illustrate the relationship between model results and parameters and is essential to improving model research comprehension [55]. Therefore, sensitivity analysis quantifies the biological reactions to any modification in the biological parameters, enabling the identification of the critical element influencing the models' output [56]. As stated in [56], several sensitivity analysis techniques have been developed for use with biological models. We use derivative-based sensitivity in our model. Partial derivatives with regard to model parameters allow for the analytical calculation of the indexes. Since R_1 and R_2 have a significant influence in determining the stability of the healthy steady state, sensitivity analysis for them is studied. The normalized forward sensitivity index of R_i, $i = 1, 2$ is given by

$$S_{\gamma}^{R_i} = \frac{\partial R_i}{\partial \gamma} \times \frac{\gamma}{R_i}, \tag{5.1}$$

where γ is given parameter.

5.2.1. *Sensitivity analysis for R_1.* By using the Eq. (5.1), sensitivity indices of R_1 to each parameter are computed as presented in Table 4. Obviously, the sensitivity analysis of R_1 do not depend in parameter's values since the sensitivity analysis with respect to any parameter is equal to 1 or -1. For instance

$$S_{\ell}^{R_1} = \frac{\partial R_1}{\partial \ell} \times \frac{\ell}{R_1} = \frac{\upsilon\nu}{\eta\varepsilon\beta} \times \frac{\ell\eta\varepsilon\beta}{\ell\upsilon\nu} = 1.$$

Table 4's representation of the sensitivity analysis's sign allows us to understand each parameter's involvement in the following ways:

- Parameters ℓ, υ and ν have positive impact on R_1. This indicates that these parameters have a role in the proliferation of KSHV throughout the body.
- On the contrary, the other parameters η, ε and β is responsible on decreasing the spread rate of KSHV in human.

These result is clearly shown in Figure 6.

TABLE 4. Sensitivity index for R_1.

Parameters γ	ℓ	υ	ν	η	ε	β
Value of $S_\gamma^{R_1}$	1	1	1	−1	−1	−1

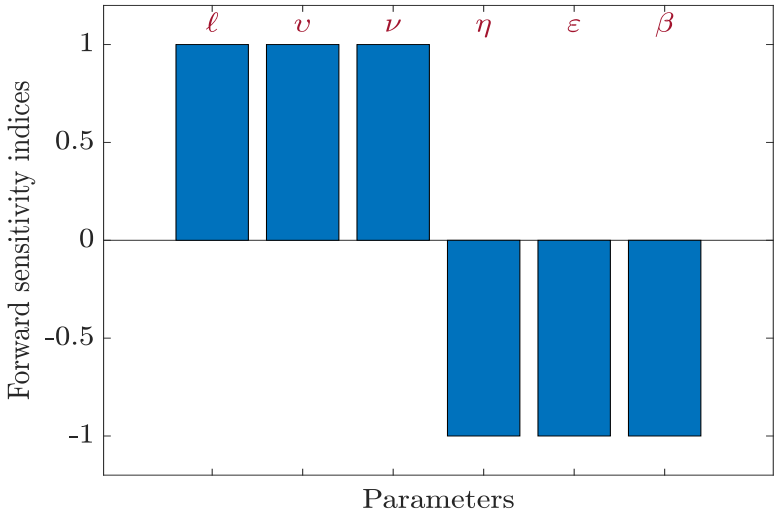

FIGURE 6. Sensitivity analysis for R_1.

5.2.2. *Sensitivity analysis for R_2.* By using the Eq. (5.1) and parameter values in Table 1, sensitivity indices of R_2 to each parameter are computed as presented in Table 5. Figure 7 illustrates the sensitivity indices values of R_2 using the parameter values in Table 1. According to the sensitivity indices that are presented in the Table 5, we have the following:

- ξ, $\varkappa$, ϱ, and β have positive indices, which mean that the increase or decrease of these parameters will increase or decrease the basic reproduction ratio for HIV-1 mono-infection R_2.
- δ, ϖ, ℓ, ϑ, and ρ have a negative impact on R_2. Thus, any increase in these values will leads to decrease the value of R_2. Clearly, δ, d, and ϑ are the most significant parameters, while ℓ and ρ are the less significant parameters.

TABLE 5. Sensitivity index for R_2.

Parameters γ	ξ	$\varkappa$	ϱ	β	δ	ϖ	ℓ	ϑ	ρ
Value of $S_\gamma^{R_2}$	1	1	1	0.0171	−1	−1	−0.0171	−0.8929	−0.0107

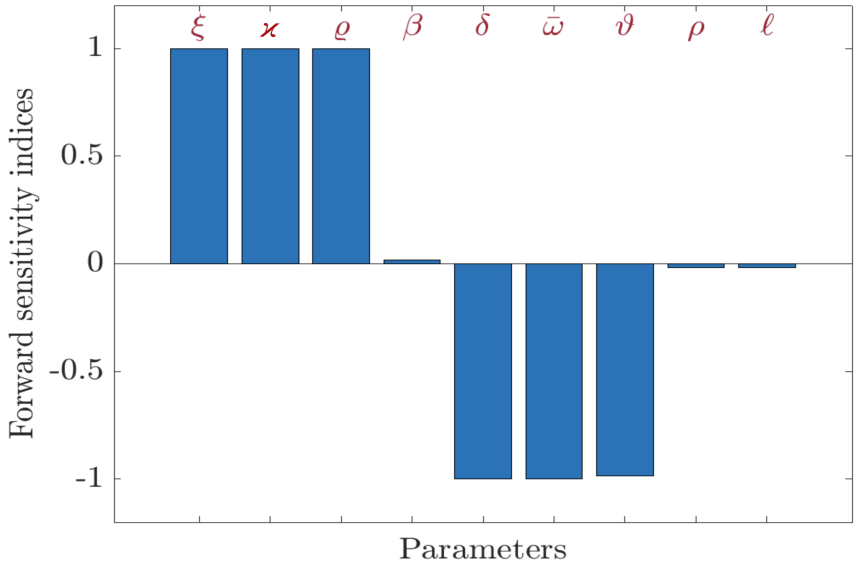

FIGURE 7. Sensitivity for R_2.

5.3. **Comparison results.** In this part, we examine the effects of KSHV or HIV-1 mono-infection on each other by comparing the dynamics of KSHV or HIV-1 co-infection with those of KSHV or HIV-1 mono-infection.

5.3.1. *Evaluation of HIV-1 co-infection with KSHV versus HIV-1 mono-infection.* We evaluate the following HIV-1 mono-infection system against the KSHV/HIV-1 co-infection model (2.1)-(2.6):

$$\dot{U} = \xi - \varpi U - \varrho UV, \tag{5.2}$$

$$\dot{Y} = \varrho UV - \delta Y, \tag{5.3}$$

$$\dot{V} = \varkappa Y - \vartheta V - \rho VW, \tag{5.4}$$

$$\dot{W} = \ell + \kappa VW - \beta W. \tag{5.5}$$

We select the parameter's values $\varrho = 0.001$ and $\nu = 0.003$ in addition to the following initial condition:

$$\textbf{Initial.4} : U(0) = 250, Y(0) = 15, V(0) = 50, W(0) = 150, Z(0) = 50, P(0) = 100.$$

The solutions of two systems (2.1)-(2.6) and (5.2)-(5.5) are displayed in Figure 8. Obviously, when HIV-1 mono-infected patients are co-infected with KSHV, then the concentrations of healthy CD4$^+$T cells are decreased while the concentrations of HIV-1 particles are increased. These findings align

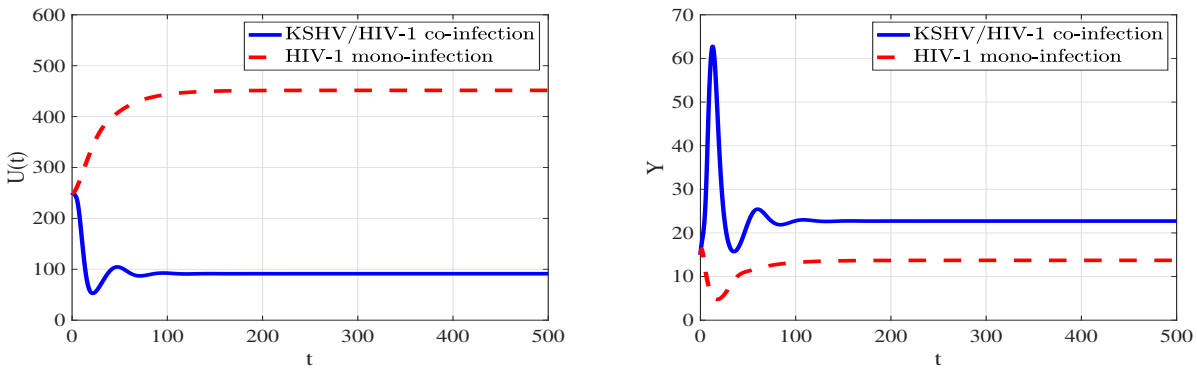

(A) Healthy CD4$^+$T cells

(B) HIV-1-infected $CD4^+T$ cells

(C) Free HIV-1 virus

(D) Healthy B cells

FIGURE 8. A comparative analysis of the models' solutions for KSHV/HIV-1 co-infection and HIV-1 mono-infection.

with research presented in [57] and [58], indicating that KSHV may increase the HIV-1 load and spread, delaying the onset of AIDS.

5.3.2. *Evaluation of HIV-1 co-infection with KSHV versus KSHV mono-infection.* We evaluate the following KSHV mono-infection system against the KSHV/HIV-1 co-infection model (2.1)-(2.6):

$$\dot{W} = \ell - \beta W - \nu WP, \tag{5.6}$$

$$\dot{Z} = \nu WP - \eta Z, \tag{5.7}$$

$$\dot{P} = \upsilon Z - \varepsilon P. \tag{5.8}$$

We choose the values $\varrho = 0.001$ and $\nu = 0.001$ and take the following initial condition as:

$$\textbf{Initial.5} : U(0) = 200, Y(0) = 300, V(0) = 50, W(0) = 100, Z(0) = 40, P(0) = 70.$$

Solutions of the two systems (2.1)-(2.6) and (5.6)-(5.8) that illustrated in Figure 9. It is evident that the B cell concentrations in both systems progressively get closer to the same value, $W_3 = W_1$. Compared to KSHV mono-infection patients, KSHV/HIV-1 co-infection patients had higher prevalence of KSHV-infected B cells and free KSHV particles. This is in line with research reported

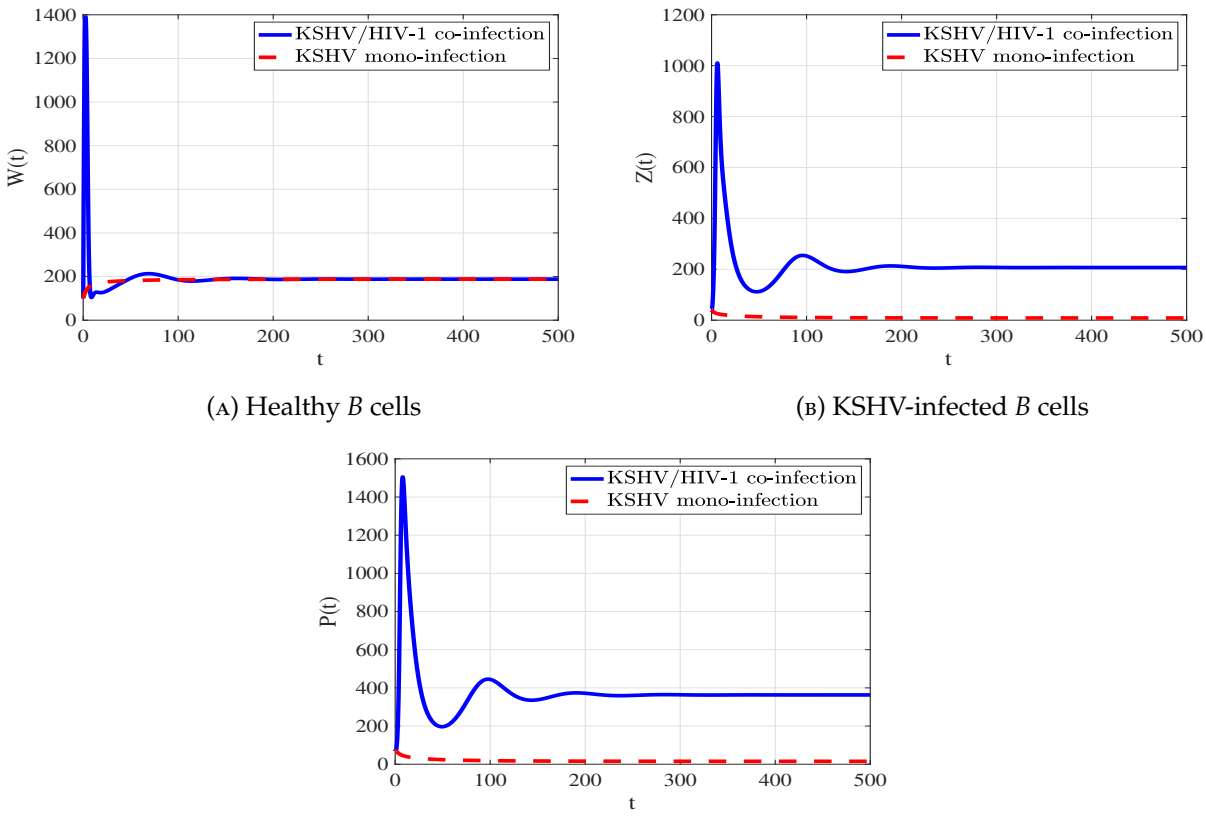

(A) Healthy B cells

(B) KSHV-infected B cells

(C) Free KSHV virus

FIGURE 9. A comparative analysis of the models' solutions for KSHV/HIV-1 co-infection and KSHV mono-infection.

in [59], which hypothesized that elevated HIV-1 DNA levels might potentially trigger KSHV reactivation by direct KSHV activation or increased immunosuppression.

6. Conclusion and discussion

By infecting CD4$^+$T cells, one of the immune system's primary components, HIV-1 damages the system and can cause AIDS. As is well known, HIV-1 is highly contagious worldwide, and those infected with it are vulnerable to opportunistic infections like KSHV. HHV8 can induce KS by attacking B cells. KSHV/HIV-1 co-infection cases have been reported recently in various nations, particularly in Africa [60–62]. In this study, we constructed and investigated a new model for KSHV and HIV-1 co-infection in a host. The interactions between healthy CD4$^+$ T cells, HIV-1-infected CD4$^+$ T cells, free HIV-1, healthy B cells, KSHV-infected B cells, and free KSHV are explained by a system of six nonlinear ODEs. First, nonnegativity and boundedness-the two main properties of the solutions-were shown. Next, we demonstrated the existence of four stable states in the model. The global asymptotic stability of the model's steady states is defined by four threshold parameters, R_i, for $i = 1, 2, 3$, and 4. We demonstrated the global asymptotic stability

for all steady state by utilizing the Lyapunov approach and LaSalle's invariance principle. Our findings are as follows:

- There is always an healthy steady state, SS_0. Additionally, when $R_1 \leq 1$ and $R_2 \leq 1$, SS_0 is GAS. An individual who is free of both KSHV and HIV-1 is represented by this case.
- There exists a KSHV mono-infection steady state SS_1 when $R_1 > 1$. Additionally, when $R_1 > 1$ and $R_3 \leq 1$, SS_1 is GAS. This condition reflects what happens to a person who just has KSHV infection.
- There exists an HIV-1 mono-infection steady state SS_2 when $R_2 > 1$. Furthermore, SS_2 is GAS when $R_2 > 1$ and $R_4 \leq 1$. This condition is representative of an individual with just HIV-1 infection.
- There exists a KSHV/HIV-1 co-infection steady state SS_3 when $R_3 > 1$ and $R_4 > 1$. Furthermore, SS_3 is GAS when $R_4 > 1$ and $1 < R_3 \leq 1 + \frac{\beta\varrho}{\omega\kappa}$. This condition is representative of an individual who carries both HIV-1 and KSHV infections.

In accordance with the theoretical outcomes, we offered numerical simulations. Sensitivity analysis was examined for both both basic reproduction ratios R_1 and R_2. A comparison was presented between co-infections of KSHV and HIV-1 and single infections of HIV-1 or KSHV. We found that the concentrations of KSHV and HIV-1 are greater when they co-infect than when they are infections apart. This result is in line with a number of findings found in the literature.

The primary constraint on our study is that we were unable to estimate the model's parameter values using actual data from patients who were co-infected with HIV-1 and KSHV. Actual data from individuals with HIV-1 or KSHV single infections may exist, but there is currently a dearth of actual data from patients who are co-infected with both HIV-1 and KSHV.

We point out that the immunological competition at the cellular level has recently been modeled using active agent techniques, see [63]. We think that our strategy can direct future advancements in agent-based techniques to accommodate the presence of various diseases. Using fractional differential equations (FDEs) to examine the effect of memory on our model's dynamics looks like an intriguing approach. FDEs have the ability to capture non-local and memory-dependent effects, which are often crucial in different biological systems. The model created in this study may also be enhanced by (i) taking viral mutations into consideration [64], (ii) utilizing real data to get an accurate estimation of the parameter values, and (iii) taking reaction-diffusion into consideration [65].

Conflicts of Interest: The authors declare that there are no conflicts of interest regarding the publication of this paper.

References

[1] N. Dorratoltaj, R. Nikin-Beers, S.M. Ciupe, S.G. Eubank, K.M. Abbas, Multi-Scale Immunoepidemiological Modeling of Within-Host and Between-Host HIV Dynamics: Systematic Review of Mathematical Models, PeerJ 5 (2017), e3877. https://doi.org/10.7717/peerj.3877.

[2] P. Aavani, L.J.S. Allen, The Role of CD4 T Cells in Immune System Activation and Viral Reproduction in a Simple Model for HIV Infection, Appl. Math. Model. 75 (2019), 210–222. https://doi.org/10.1016/j.apm.2019.05.028.

[3] S.L. Swain, K.K. McKinstry, T.M. Strutt, Expanding Roles for CD4+ T Cells in Immunity to Viruses, Nat. Rev. Immunol. 12 (2012), 136–148. https://doi.org/10.1038/nri3152.

[4] D. Wodarz, D.N. Levy, Human Immunodeficiency Virus Evolution Towards Reduced Replicative Fitnessin Vivoand the Development of AIDS, Proc. R. Soc. B. 274 (2007), 2481–2491. https://doi.org/10.1098/rspb.2007.0413.

[5] P.L. Vernazza, J.J. Eron, S.A. Fiscus, M.S. Cohen, Sexual Transmission of HIV: Infectiousness and Prevention, AIDS 13 (1999), 155–166. https://doi.org/10.1097/00002030-199902040-00003.

[6] T.F. Schulz, Y. Chang, P.S. Moore, Kaposi's Sarcoma-Associated Herpesvirus (Human Herpesvirus 8), in: D.J. McCance (Ed.), Human Tumor Viruses, ASM Press, Washington, DC, USA, 2014: pp. 87–134. https://doi.org/10.1128/9781555818289.ch3.

[7] Y. Chang, E. Cesarman, M.S. Pessin, F. Lee, J. Culpepper, D.M. Knowles, P.S. Moore, Identification of Herpesvirus-Like DNA Sequences in AIDS-Sssociated Kaposi's Sarcoma, Science 266 (1994), 1865–1869. https://doi.org/10.1126/science.7997879.

[8] S.M. Akula, F.Z. Wang, J. Vieira, B. Chandran, Human Herpesvirus 8 Interaction With Target Cells Involves Heparan Sulfate, Virology 282 (2001), 245–255. https://doi.org/10.1006/viro.2000.0851.

[9] S.J. Dollery, R.J. Santiago-Crespo, D. Chatterjee, E.A. Berger, Glycoprotein K8.1A of Kaposi's Sarcoma-Associated Herpesvirus Is a Critical B Cell Tropism Determinant Independent of Its Heparan Sulfate Binding Activity, J. Virol. 93 (2019), 01876-18. https://doi.org/10.1128/jvi.01876-18.

[10] R.F. Kaondera-Shava, E. Lungu, B. Szomolay, A Novel Mathematical Model of AIDS-Associated Kaposi's Sarcoma: Analysis and Optimal Control, Biosystems. 200 (2021), 104318. https://doi.org/10.1016/j.biosystems.2020.104318.

[11] M.J. Cannon, A.S. Laney, P.E. Pellett, Human Herpesvirus 8: Current issues, Clinic. Infect. Dis. 37 (2003), 82–87. https://doi.org/10.1086/375230.

[12] E. Rohner, N. Wyss, Z. Heg, Z. Faralli, S.M. Mbulaiteye, U. Novak, M. Zwahlen, M. Egger, J. Bohlius, HIV and Human Herpesvirus 8 Co-Infection Across the Globe: Systematic Review and Meta-Analysis, Int. J. Cancer. 138 (2015), 45–54. https://doi.org/10.1002/ijc.29687.

[13] L.C. Pierrotti, A. Etzel, L.M. Sumita, P.E. Braga, J. Eluf-Neto, V.A.U.F. de Souza, A.A.C. Segurado, Human Herpesvirus 8 (HHV-8) Infection in HIV/AIDS Patients from Santos, Brazil: Seroprevalence and Associated Factors, Sex. Transmitted Dis. 32 (2005), 57–63. https://doi.org/10.1097/01.olq.0000148300.33428.6e.

[14] M. Maskew, A.P. MacPhail, D. Whitby, M. Egger, C.L. Wallis, M.P. Fox, Prevalence and Predictors of Kaposi Sarcoma Herpes Virus Seropositivity: A Cross-Sectional Analysis of HIV-Infected Adults Initiating ART in Johannesburg, South Africa, Infect. Agents Cancer. 6 (2011), 22. https://doi.org/10.1186/1750-9378-6-22.

[15] M. Masiá, C. Robledano, V. Ortiz de la Tabla, P. Antequera, B. Lumbreras, I. Hernández and F. Gutiérrez, Coinfection With Human Herpesvirus 8 Is Associated With Persistent Inflammation and Immune Activation in Virologically Suppressed HIV-Infected Patients, PLoS ONE. 9 (2014), e105442. https://doi.org/10.1371/journal.pone.0105442.

[16] D. Oktafiani, N.L. Megasari, E. Fitriana, N. Nasronudin, M.I. Lusida, S. Soetjipto, Detection of Human Herpesvirus-8 Antigen in HIV-Infected Patients in East Java, Indonesia, Afr. J. Infect. Dis. 12 (2018), 43–46. https://doi.org/10.21010/ajid.v12i2.7.

[17] D. Watanabe, S. Iida, K. Hirota, T. Ueji, T. Matsumura, Y. Nishida, T. Uehira, H. Katano, T. Shirasaka, Evaluation of Human Herpesvirus-8 Viremia and Antibody Positivity in Patients with HIV Infection With Human Herpesvirus-8-related Diseases, J. Med. Virol. 95 (2023), e29324. https://doi.org/10.1002/jmv.29324.

[18] H. Lambarey, M.J. Blumenthal, A. Chetram, W. Joyimbana, L. Jennings, C. Orrell, G. Schäfer, Reactivation of Kaposi's Sarcoma-Associated Herpesvirus (KSHV) by SARS-CoV-2 in Non-hospitalised HIV-Infected Patients, eBioMedicine. 100 (2024), 104986. https://doi.org/10.1016/j.ebiom.2024.104986.

[19] M.A. Nowak, C.R.M. Bangham, Population Dynamics of Immune Responses to Persistent Viruses, Science. 272 (1996), 74–79. https://doi.org/10.1126/science.272.5258.74.

[20] A.V. Herz, S. Bonhoeffer, R.M. Anderson, R.M. May, M.A. Nowak, Viral Dynamics in Vivo: Limitations on Estimates of Intracellular Delay and Virus Decay, Proc. Nat. Acad. Sci. U.S.A. 93 (1996), 7247–7251. https://doi.org/10.1073/pnas.93.14.7247.

[21] R.V. Culshaw, S. Ruan, A Delay-Differential Equation Model of HIV Infection of CD4+ T-Cells, Math. Biosci. 165 (2000), 27–39. https://doi.org/10.1016/s0025-5564(00)00006-7.

[22] P.W. Nelson, A.S. Perelson, Mathematical Analysis of Delay Differential Equation Models of HIV-1 Infection, Math. Biosci. 179 (2002), 73–94. https://doi.org/10.1016/s0025-5564(02)00099-8.

[23] Z. Li, X.Q. Zhao, Global Dynamics of a Time-Delayed Nonlocal Reaction-Diffusion Model of Within-Host Viral Infections, J. Math. Biol. 88 (2024), 38. https://doi.org/10.1007/s00285-024-02052-5.

[24] J. Lin, R. Xu, X. Tian, Threshold Dynamics of an Hiv-1 Virus Model With Both Virus-to-Cell and Cell-to-Cell Transmissions, Intracellular Delay, and humoral immunity, Appl. Math. Comp. 315 (2017), 516–530. https://doi.org/10.1016/j.amc.2017.08.004.

[25] Y. Gao, J. Wang, Threshold Dynamics of a Delayed Nonlocal Reaction-Diffusion HIV Infection Model With Both Cell-Free and Cell-to-Cell Transmissions, J. Math. Anal. Appl. 488 (2020), 124047. https://doi.org/10.1016/j.jmaa.2020.124047.

[26] Z. Zhu, R. Wu, Y. Yang, Y. Xu, Modelling HIV Dynamics With Cell-to-cell Transmission and CTL Response, Math. Methods Appl. Sci. 46 (2022), 6506–6528. https://doi.org/10.1002/mma.8921.

[27] J. Li, X. Wang, Y. Chen, Analysis of an Age-Structured HIV Infection Model With Cell-to-Cell Transmission, Eur. Phys. J. Plus 139 (2024), 78. https://doi.org/10.1140/epjp/s13360-024-04873-1.

[28] R. Xu, C. Song, Dynamics of an HIV Infection Model With Virus Diffusion and Latently Infected Cell Activation, Nonlinear Anal.: Real World Appl. 67 (2022), 103618. https://doi.org/10.1016/j.nonrwa.2022.103618.

[29] A.S. Perelson, P. Essunger, Y. Cao, M. Vesanen, A. Hurley, K. Saksela, M. Markowitz, D.D. Ho, Decay Characteristics of HIV-1-Infected Compartments During Combination Therapy, Nature 387 (1997), 188–191. https://doi.org/10.1038/387188a0.

[30] K. Hattaf, H. Dutta, Modeling the Dynamics of Viral Infections in Presence of Latently Infected Cells, Chaos Solitons Fractals. 136 (2020), 109916. https://doi.org/10.1016/j.chaos.2020.109916.

[31] Y. Wang, Y. Zhou, F. Brauer, J.M. Heffernan, Viral Dynamics Model With CTL Immune Response Incorporating Antiretroviral Therapy, J. Math. Biol. 67 (2012), 901–934. https://doi.org/10.1007/s00285-012-0580-3.

[32] D. Wodarz, R.M. May, M.A. Nowak, The Role of Antigen-Independent Persistence of Memory Cytotoxic T Lymphocytes, Int. Immunol. 12 (2000), 467–477. https://doi.org/10.1093/intimm/12.4.467.

[33] Z. Xie, X. Liu, Global Dynamics in an Age-Structured HIV Model With Humoral Immunity, Int. J. Biomath. 14 (2021), 2150047. https://doi.org/10.1142/s1793524521500479.

[34] D. Wodarz, Hepatitis C Virus Dynamics and Pathology: The Role of CTL and Antibody Responses, J. Gen. Virol. 84 (2003), 1743–1750. https://doi.org/10.1099/vir.0.19118-0.

[35] P. Dubey, U.S. Dubey, B. Dubey, Modeling the Role of Acquired Immune Response and Antiretroviral Therapy in the Dynamics of HIV Infection, Math. Comp. Simul. 144 (2018), 120–137. https://doi.org/10.1016/j.matcom.2017.07.006.

[36] Z. Zhang, Y. Chen, X. Wang, L. Rong, Dynamic Analysis of a Latent HIV Infection Model With CTL Immune and Antibody Responses, Int. J. Biomath. 17 (2023), 2350079 https://doi.org/10.1142/s1793524523500791.

[37] G. Huang, X. Liu, Y. Takeuchi, Lyapunov Functions and Global Stability for Age-Structured HIV Infection Model, SIAM J. Appl. Math. 72 (2012), 25–38. https://doi.org/10.1137/110826588.

[38] J. Wang, J. Lang, X. Zou, Analysis of an Age Structured HIV Infection Model With Virus-to-Cell Infection and Cell-to-Cell Transmission, Nonlinear Anal.: Real World Appl. 34 (2017), 75–96. https://doi.org/10.1016/j.nonrwa.2016.08.001.

[39] L. Rong, A.S. Perelson, Modeling Latently Infected Cell Activation: Viral and Latent Reservoir Persistence, and Viral Blips in HIV-Infected Patients on Potent Therapy, PLoS Comp. Biol. 5 (2009), e1000533. https://doi.org/10.1371/journal.pcbi.1000533.

[40] A. Mojaver, H. Kheiri, Mathematical Analysis of a Class of HIV Infection Models of CD4+ T-Cells With Combined Antiretroviral Therapy, Appl. Math. Comp. 259 (2015), 258–270. https://doi.org/10.1016/j.amc.2015.02.064.

[41] B.J. Nath, K. Sadri, H.K. Sarmah, K. Hosseini, An Optimal Combination of Antiretroviral Treatment and Immunotherapy for Controlling HIV Infection, Math. Comp. Simul. 217 (2024), 226–243. https://doi.org/10.1016/j.matcom.2023.10.012.

[42] O.M. Chimbola, E.M. Lungu, B. Szomolay, Optimal Control Application to a Kaposi's Sarcoma Treatment Model, Int. J. Biomath. 15 (2022), 2150081. https://doi.org/10.1142/s1793524521500819.

[43] F. Nani, M. Jin, Dynamics of HIV-1 Associated Kaposi Sarcoma during HAART Therapy, Math and Computer Science Faculty Working Papers, 20, (2011).

[44] F. Nani, M. Jin, Analysis of Dynamics of HIV-1 Associated Kaposi Sarcoma during HAART and ACI, Br. J. Math. Comp. Sci. 19 (2016), 1–22. https://doi.org/10.9734/bjmcs/2016/20358.

[45] B. Szomolay, E.M. Lungu, A Mathematical Model for the Treatment of Aids-Related Kaposi's Sarcoma, J. Biol. Syst. 22 (2014), 495–522. https://doi.org/10.1142/s0218339014500247.

[46] O.M. Chimbola, E.M. Lungu, B. Szomolay, Effect of Innate and Adaptive Immune Mechanisms on Treatment Regimens in an Aids-Related Kaposi's Sarcoma Model, J. Biol. Dyn. 15 (2021), 213–249. https://doi.org/10.1080/17513758.2021.1912420.

[47] A.S. Perelson, D.E. Kirschner, R. De Boer, Dynamics of HIV Infection of CD4+ T Cells, Math. Biosci. 114 (1993), 81–125. https://doi.org/10.1016/0025-5564(93)90043-a.

[48] M.M. Hadjiandreou, R. Conejeros, V.S. Vassiliadis, Towards a Long-Term Model Construction for the Dynamic Simulation of HIV Infection, Math. Biosci. Eng. 4 (2007), 489–504. https://doi.org/10.3934/mbe.2007.4.489.

[49] S.K. Sahani, Yashi, Effects of Eclipse Phase and Delay on the Dynamics of HIV Infection, J. Biol. Syst. 26 (2018), 421–454. https://doi.org/10.1142/s0218339018500195.

[50] O.M. Chimbola, Mathematical Model of Classical Kaposi's Sarcoma, Appl. Math. 11 (2020), 579–600. https://doi.org/10.4236/am.2020.117040.

[51] H.L. Smith, P. Waltman, The Theory of the Chemostat: Dynamics of Microbial Competition, Cambridge University Press, 1995.

[52] A. Korobeinikov, Global Properties of Basic Virus Dynamics Models, Bull. Math. Biol. 66 (2004), 879–883. https://doi.org/10.1016/j.bulm.2004.02.001.

[53] J.K. Hale, S.M.V. Lunel, Introduction to Functional Differential Equations, Springer, New York, (1993).

[54] H.K. Khalil, Nonlinear Systems, 3rd Edition, Prentice Hall, Upper Saddle River, (2002).

[55] M. Renardy, C. Hult, S. Evans, J.J. Linderman, D.E. Kirschner, Global Sensitivity Analysis of Biological Multiscale Models, Curr. Opinion Biomed. Eng. 11 (2019), 109–116. https://doi.org/10.1016/j.cobme.2019.09.012.

[56] Z. Zi, Sensitivity Analysis Approaches Applied to Systems Biology Models, IET Syst. Biol. 5 (2011), 336–346. https://doi.org/10.1049/iet-syb.2011.0015.

[57] V.M.S. de Morais, E.L.S. de Lima, G.G.d.M. Cahú, et al. MBL2 Gene Polymorphisms in HHV-8 Infection in People Living with HIV/AIDS, Retrovirology, 15 (2018), 75. https://doi.org/10.1186/s12977-018-0456-8.

[58] R. Minami, M. Yamamoto, S. Takahama, H. Ando, T. Miyamura, E. Suematsu, Human Herpesvirus 8 DNA Load in the Leukocytes Correlates with the Platelet Counts in HIV Type 1-Infected Individuals, AIDS Res. Human Retrovir. 25 (2009), 1–8. https://doi.org/10.1089/aid.2007.0260.

[59] R. Tedeschi, M. Enbom, E. Bidoli, A. Linde, P. De Paoli, J. Dillner, Viral Load of Human Herpesvirus 8 in Peripheral Blood of Human Immunodeficiency Virus-Infected Patients with Kaposi's Sarcoma, J. Clin. Microbiol. 39 (2001), 4269–4273. https://doi.org/10.1128/jcm.39.12.4269-4273.2001.

[60] A. Caterino-de-Araujo, R.C.R. Manuel, R. Del Bianco, E. Santos-Fortuna, M.C. Magri, J.M.K. Silva, R. Bastos, Seroprevalence of Human Herpesvirus 8 Infection in Individuals From Health Care Centers in Mozambique: Potential for Endemic and Epidemic Kaposi's Sarcoma, J. Med. Virol. 82 (2010), 1216–1223. https://doi.org/10.1002/jmv.21789.

[61] L.G. Chatlynne, D.V. Ablashi, Seroepidemiology of Kaposi's Sarcoma-Associated Herpesvirus (KSHV), Semin. Cancer Biol. 9 (1999), 175–185. https://doi.org/10.1006/scbi.1998.0089.

[62] S.M. Mbulaiteye, R.M. Pfeiffer, D. Whitby, G.R. Brubaker, J. Shao, R.J. Biggar, Human Herpesvirus 8 Infection within Families in Rural Tanzania, J. Infect. Dis. 187 (2003), 1780–1785. https://doi.org/10.1086/374973.

[63] D. Burini, D.A. Knopoff, Epidemics and Society – a Multiscale Vision from the Small World to the Globally Interconnected World, Math. Models Methods Appl. Sci. 34 (2024), 1567–1596. https://doi.org/10.1142/s0218202524500295.

[64] N. Bellomo, D. Burini, N. Outada, Multiscale Models of Covid-19 with Mutations and Variants, Netw. Heterog. Media, 17 (2022), 293–310. https://doi.org/10.3934/nhm.2022008.

[65] N. Bellomo, K.J. Painter, Y. Tao, M. Winkler, Occurrence vs. Absence of Taxis-Driven Instabilities in a May–Nowak Model for Virus Infection, SIAM J. Appl. Math. 79 (2019), 1990–2010. https://doi.org/10.1137/19m1250261.